

# We are IntechOpen, the world's leading publisher of Open Access books Built by scientists, for scientists

6,900

Open access books available

186,000

International authors and editors

200M

Downloads

Our authors are among the

154

Countries delivered to

TOP 1%

most cited scientists

12.2%

Contributors from top 500 universities



WEB OF SCIENCE™

Selection of our books indexed in the Book Citation Index  
in Web of Science™ Core Collection (BKCI)

Interested in publishing with us?  
Contact [book.department@intechopen.com](mailto:book.department@intechopen.com)

Numbers displayed above are based on latest data collected.  
For more information visit [www.intechopen.com](http://www.intechopen.com)



# Probing Biological Water Using Terahertz Absorption Spectroscopy

*Rajib Kumar Mitra and Dipak Kumar Palit*

## Abstract

Hydrogen bonding properties of water molecules, which are confined in microcavities of biological interfaces, are significantly different from those of bulk water and drive most of the complex biological processes. While NMR, X-ray and UV-vis-IR spectroscopic techniques have been found inadequate for describing the dynamics of the thick (20–40 Å) sheath of hydration layer around biomolecules, recently developed THz spectroscopy has emerged as a powerful technique to directly probe the collective dynamics of hydrogen bonds in the hydration layer, which control all important functions of the biomolecules in life. Both laser and accelerator-based THz sources are intense enough to penetrate up to about 100 μm thick water samples, which makes THz transmission and/or dielectric relaxation measurements possible in aqueous solutions. These measurements provide valuable information about the rattling and rotational motions of hydrated ions, making, breaking and rearrangement of hydrogen bonds in hydration layer as well as hydrophilic and hydrophobic interactions between biomolecule and water. THz spectroscopy has also been successfully applied to study the effect of modulation of the physical conditions, like temperature, pH, concentration of proteins and chemical additives, on the structure and dynamics of hydration layer. THz spectroscopy has also been applied to study the processes of denaturation, unfolding and aggregation of biomolecules.

**Keywords:** Hydration Layer, Biomolecules, Hydrogen bond reorganization dynamics, THz spectroscopy, Protein aggregation

## 1. Introduction

Water molecules, which reside on the surfaces of proteins or lipid bilayers or in tissues and cells, exhibit properties that are significantly different from those found in pure or bulk water as water molecules in such biological systems face additional interactions [1–7]. Unique properties of such water molecules, which are confined in microenvironments of biological surfaces or interfaces are popularly termed as ‘biological water’. This water drives many biological processes, in which it plays wide varieties of roles at different levels of complexity making its participation increasingly evident as an active agent and not simply as the spectator solvent [8–12]. Biological water differs from bulk water in a number of ways. First, clustering of the water molecules at the surface of a protein increases the local density by as much as 25% compared to that in bulk water [13, 14]. MD simulation by Smith

et al. has revealed that about half of this density increase arises from the shortening of the average water – water distances and the other half from an increase in the coordination number [15]. Second, replacement of the water–water hydrogen bonds by the water–protein hydrogen bonds in the protein hydration layer lowers the freezing point of the hydration water (i.e. prevents formation of ice). The hydration layer of many proteins does not freeze even at sub-zero temperatures and thus life may sustain even at low temperatures [16–18]. Third, in bulk water, mutual polarization of the hydrogen bonded water molecules increases the dipole moment and dielectric constant. Such polarization is absent for water molecules in hydration layers of biological molecules, i.e. biological water is less polar than bulk water [19]. Further, measurements of water dynamics suggest that around 10–25% of water molecules in cells have slower reorientation dynamics, by around an order of magnitude, than those in the bulk [2, 20]. Centrality of liquid water to life can be easily understood from the fact that condition for the search for the possibility of life elsewhere is the presence of trace of water [21]. In spite of this status, role of water in sustaining life is still not understood perfectly [12]. It is now, however, clear that water plays an active role in the life of the cell over many scales of time and distance and exhibits diverse structural and dynamical roles in molecular cell biology [3, 22].

In liquid (or bulk) water, the molecules form a tetrahedrally coordinated motif, which is the building block of ephemeral six-membered (ice-like) or five-membered (clathrate-like) ring structure, consisting of fluctuating network of hydrogen bonds, but each bond has an average lifetime of about a picosecond [23]. Thermodynamics of hydration in water are generally governed by a balance between the enthalpic and entropic consequences, namely the enthalpies of water–water and water–solute interactions (hydrogen bonding, electrostatic, and van der Waals) and the entropies of disrupting the relatively ordered hydrogen-bonded networks of bulk water and forming new hydrogen bonds to suit the geometric factors of the biological interfaces [15, 24, 25].

Similarities in water dynamics in hydration shells of various proteins [26] suggest that the dynamics are determined by rather general features of surface chemistry and topology, which induce excluded volume effects and hinder the approach of new hydrogen bond acceptors within the hydration network. There is now universal recognition that the dynamical behavior of biological macromolecules cannot be decoupled from that of water and the dynamical behavior of the hydration shell largely controls the chemical function of the biological molecules [27, 28].

Since the development of this understanding that biomolecules are surrounded by a sheath of hydration water, which takes active part in all of their normal activities, extensive efforts have been made to perceive the detailed structure and dynamics of the hydration layer using a variety of spectroscopic methods, such as X-ray and neutron scattering [14, 29, 30], NMR [31–33], second harmonic generation [34, 35] and ultrafast fluorescence and IR spectroscopies [1, 2, 22, 26, 36, 37], assisted by *ab initio* and molecular dynamics simulations [24, 25, 38, 39]. However, these measurements could provide information about the dynamics of water and the biomolecules at a low-hydration level corresponding to the first layer of hydration water only. Since fluctuations of protein and solvent dynamics take place over a wide range of length scales (in the range of a few nm) and timescales (from milliseconds to picoseconds) influencing several aspects of protein function, no single technique can span so many spatial and temporal orders of magnitude. Therefore, there has obviously been a debate about how to reconcile the results of different experimental methods that explore dynamics [1, 2, 22, 40, 41].

Recent realization that low-frequency and large-amplitude modes of water molecules in the hydration shell are particularly important in controlling the

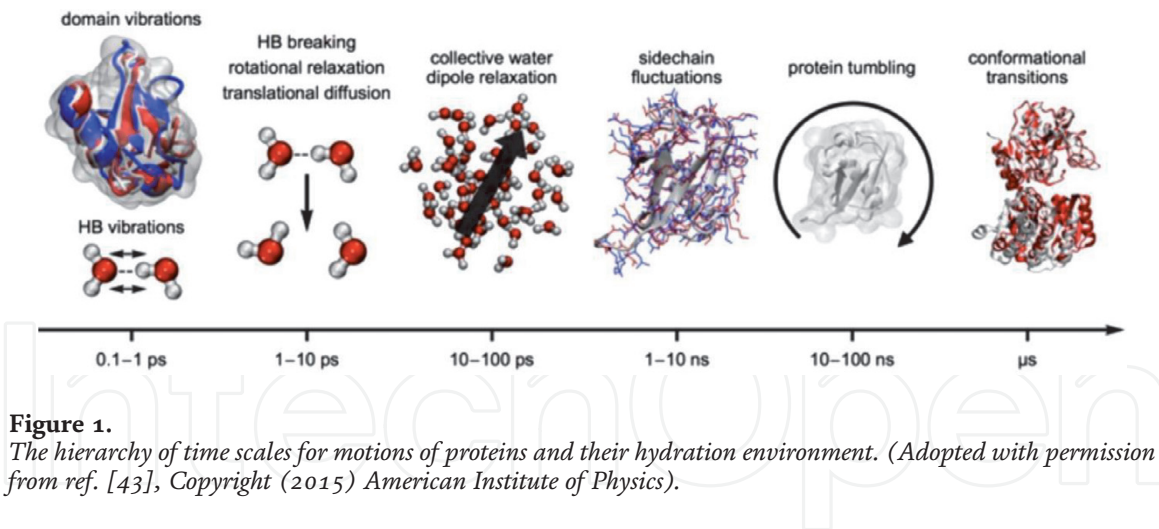


**Figure 1.** The hierarchy of time scales for motions of proteins and their hydration environment. (Adopted with permission from ref. [43], Copyright (2015) American Institute of Physics).

conformational changes that dominate protein function, has led to using the terahertz (THz) spectroscopy to observe water dynamics around biological molecules [42, 43]. THz radiation ( $1 \text{ THz} = 10^{12} \text{ Hz} = 33.33 \text{ cm}^{-1}$ ) excites the low frequency vibrations of the solvated protein and directly probes the collective hydrogen bond dynamics of the coupled protein-water system in (sub-) ps time domain. Librational, translational and intermolecular, collective motions of hydration water, as well as large amplitude motions of biomolecules, also occur in similar time scale (see **Figure 1**). In frequency domain, this corresponds to low-frequency modes in the 1–10 THz frequency region. In spite of the fact that water molecules strongly attenuate the THz radiation in this frequency region, laser or accelerator-based THz sources (vide Section 2) are now powerful enough to penetrate water layers. Modern THz spectroscopic techniques can provide valuable information about water dynamics in the frequency region of the electromagnetic spectrum ( $0.3\text{--}20 \text{ THz}$  or  $10 \text{ to } 600 \text{ cm}^{-1}$ , the so-called “terahertz gap” between the dielectric and the infrared regimes). This has offered a unique view of the hydration water in fully solvated biomolecules.

## 2. THz transmission or absorption spectroscopy

Two kinds of THz spectroscopy techniques, namely THz transmission and THz time-domain spectroscopy (THz-TDS), have extensively been used to record the THz absorption spectra of biological materials. THz transmission spectroscopy is a simple single or dual beam steady state spectrometer using THz radiation beam to estimate the THz absorption coefficient. THz transmission or absorption spectroscopy of fully solvated biomolecules in water yields direct information on the global dynamical correlations among solvent (water) molecules. However, application of THz spectroscopy to study solvated biomolecules was not possible because of huge absorption of water in the THz frequency range. This problem was solved by the development of the p-Ge laser, which was a strong the THz emitter [44–47]. Prior to this development, weak radiation power of standard sources like a globar or an arc lamp in the far IR and THz region was the cause for poor signal to noise ratio and the measurements were limited to powders or hydrated films of biomolecules, but not in their native aqueous environment. Free-electron lasers [48, 49] and synchrotrons [50], which are also sources of high power far-IR and THz pulses, have also been reported to be used for spectroscopy studies of biomolecules but are not easily accessible. THz transmission spectroscopy of water in biological systems received a momentum after the discovery of the p-Ge laser. This laser is a powerful

table-top THz source (up to about 400 W) and has the tunability in the 80–100  $\text{cm}^{-1}$  (2.4–3.3 THz) frequency region. Development of a table top dual beam (reference and sample arms) THz transmission spectrometer ensured accurate measurements of absorption of water of thickness as large as 100  $\mu\text{m}$  [51].

Accelerators delivering ultrashort pulses of relativistic electrons have been widely used as a source of high intensity THz radiation. Free electron lasers and synchrotrons are actually seeded by short duration electron pulses. An easier method of generating high intensity and tuneable THz radiation using an ultrafast electron accelerator is the coherent transition radiation (CTR). CTR occurs when a charged particle passes through an interface between media with different dielectric constants [52–55]. Sudden change in the dielectric constants along the electron's path causes a discontinuity in the electric field at the interface and this discontinuity readjusts itself as radiation spreading out from the point where the electron passes through the discontinuity. The angular spectral energy density of the CTR depends on the dielectric constants of the two media [56, 57]. Since the dielectric constants of aluminum and gold are much more than that of vacuum in far-IR region, these two metals are frequently used as perfect conductors. Direction of propagation and the intensity distribution of the CTR with respect to the angle of incidence of the electron pulse on the target has been discussed in detail in Ref. [53].

At wavelengths shorter than the bunch length, the emitted radiation field is incoherent and total intensity is proportional to the number of electrons ( $N$ ). But at wavelengths longer than the electron bunch length, the radiation emitted from the bunch is coherent. With a typical number of electrons per bunch on the order of  $10^8$ – $10^9$ , the coherent radiation intensity greatly exceeds that of incoherent radiation. Especially, at long wavelengths compared to the bunch length, the radiation intensity is proportional to the square of the number of electrons in the bunch. Therefore, it is possible to generate coherent radiation in the far-IR or THz spectral range from short electron bunches with bunch lengths of hundred micron or less. Moreover, the shorter the bunch length, the broader is the radiation spectrum that can be generated. With larger number of electrons in the bunch, the total intensity (both coherent and incoherent components) of the CTR at frequency  $\omega$  is given by,

$$I_{total}(\omega) = NI_e(\omega)(N - 1)[1 + (N - 1)f(\omega)] \quad (1)$$

In this equation, contribution of the coherent component,  $I_{coherent}(\omega)$ , is given by,

$$I_{coherent}(\omega) = N(N - 1)I_e(\omega)f(\omega) \quad (2)$$

Here,

$$f(\omega) = e^{-\left(\frac{\omega\sigma_z}{c}\right)^2} \quad (3)$$

and  $I_e(\omega)$  is the radiation intensity generated from one electron in the bunch and Eqs. (1) and (2) have been derived assuming that all electrons in the bunch have the same energy.  $f(\omega)$  is the bunch form factor at frequency  $\omega$ , and it is the absolute square of Fourier transformation of the normalized bunch distribution.  $\sigma_z$  is the Gaussian bunch width in  $\mu\text{m}$ . Moreover, the shorter the bunch length, the broader is the radiation spectrum that can be generated. The Gaussian electron bunches with bunch lengths of 100, 200 and 300 fs can provide broadband radiation spectra covering the wavenumbers up to about 220, 110 and 70  $\text{cm}^{-1}$  (or 6.6, 3.33 and 2.1 THz), respectively [55].

In THz transmission measurements at AIST, Tsukuba, Japan, a femtosecond linear accelerator system, which delivered electron pulses of about 300 fs duration,

and electron energy of 42 MeV and  $\sim 100$  pC charge ( $\sim 10^8$  electrons per one macro-pulse) [58], was used. Electron beam was directed to hit a thin gold foil (thickness is about 500  $\mu\text{m}$ ) at an incidence angle of  $45^\circ$ . CTR, which contained the component of THz radiation, was collected in the direction perpendicular to the electron beam using a gold coated parabolic mirror and the intensity of the THz radiation was measured using a Schottky diode detector [54]. Intensity of the THz pulse generated by this method was of high intensity (about 100 nJ/micropulse and covered a wide frequency range (0.3–2.5 THz), which was practically determined by the frequency response of the Schottky diode detector. Band pass filters (Tydex, Russia) were used to select a band of THz frequencies for estimation of absorption of protein solutions. Absorbance of the solutions of different path lengths were measured. Samples were taken in Bruker liquid sample cells, path lengths of which were varied using Teflon spacers of required thicknesses. Fused silica windows having thickness of 1.5 mm were used in the Bruker sample cell. Thicknesses of the Teflon spacers used were in the range of 20 to 150  $\mu\text{m}$ . Absorption coefficient value (in  $\text{cm}^{-1}$ ) of the solution was estimated from the slope of the linear plot of absorbance vs. path length of the cell (Eq. (4)) [59]. Experimental arrangement used here corresponded to that of a single beam absorption spectrometer.

$$\ln \left( \frac{I_0}{I_d} \right) = \alpha_{\text{sol}} d \quad (4)$$

Here,  $I_0$  and  $I_d$  represent the beam intensities in the absence (i.e. using the blank cell) and presence of the sample solution, respectively.  $\alpha_{\text{sol}}$  represents the absorption coefficient of the sample solution,  $d$  is the path length or thickness of the sample.

The absorption coefficient of the sample,  $\alpha$ , is defined by,

$$\alpha = \frac{4\pi\bar{\nu}k}{c} \quad (5)$$

$\bar{\nu}$  ( $\text{cm}^{-1}$ ) is the frequency of THz radiation,  $k$  is the imaginary part of the complex refractive index and  $c$  is the speed of light. The complex refractive index is defined as,

$$\bar{n}(\bar{\nu}) = n(\bar{\nu}) + i k(\bar{\nu}) \quad (6)$$

The real part  $n(\bar{\nu})$  describes the refractive index of the sample, while the imaginary part  $k$  is the absorption.

Presently, the THz-TDS in the 0.1–10 THz ( $3.33 \text{ cm}^{-1}$ – $333 \text{ cm}^{-1}$ ) region is the most popular technique, which has been extensively applied in the fields of research in chemistry, materials science, physics, engineering, medicine as well as in industry [60–74]. THz-TDS has also been proved to be a valuable technique for investigation of low frequency dielectric relaxation and vibrational spectroscopy of hydrogen bonded liquids, such as water, alcohols, and others [75–77]. While various configurations of the THz time-domain spectrometer have been used depending on the kind of applications, we will describe here the general principle of the technique and the spectrometer configuration used for investigation of biomolecules.

The core principle of the THz-TDS technique, which uses a short duration (say a few tens of femtosecond) pulses of THz radiation, is measurement of the transient electric field associated with the THz pulse rather than variation of intensity of the frequency components of the THz pulse. However, since the response or the rise times of the electronic components and detectors are slower than a few ps, it is the normal practice to use the pump-and-probe kind of optical configurations in

ultrafast spectrometers in order to overcome the slow response of the detectors. To achieve sub-picosecond time resolution in THz-TDS, the ultrashort NIR optical pulse (typically shorter than 100 fs) is beam-split along two paths to generate pump and probe pulses and to detect the time dependent THz field using a time-delay stage. Schematic diagram presented in **Figure 2** represents the principle of a THz-time-domain spectrometer.

The pump pulse, which contains the major amount of energy (more than 70% of the total energy of the laser beam), is used for generating broadband pulses of THz radiation using a photoconductive antenna consisting of a low temperature grown GaAs or InGaAs film covered with metallic contacts for application of bias voltage, or by optical rectification in ZnTe(110) crystal. The pulsed beam of THz radiation is collimated and focused onto the sample using gold coated parabolic mirrors. After transmission through the sample, the THz beam is recollimated and refocused on another photoconductive antenna or ZnTe(110) crystal, which works as the THz detector. Recently, ZnTe (110) crystal are being used extensively both as THz emitter as well as in detection because of possibility of its application in much wider THz frequency region as compared to that has been possible using photoconductive antenna.

The probe beam is used to gate the detector and measure the instantaneous THz electric field using the method of electro-optic sampling. A high precision linear motion stage is used to delay the probe pulses to arrive at detector crystal with respect to the pump pulses. The THz pulse and the gate (NIR) pulse are propagated collinearly through the ZnTe crystal. The THz pulse induces a birefringence in ZnTe crystal, which is read out by a linearly polarized gate pulse. When both the gate pulse and the THz pulse are present in the crystal at the same time, the polarization of the gate pulse will be rotated by the THz pulse depending on the strength of the electric field of the THz pulse. Using a  $\lambda/4$  waveplate and a beam splitting polarizer together with a set of balanced photodiodes, the THz pulse amplitude is mapped by monitoring the gate pulse polarization rotation after the ZnTe crystal at various delay times with respect to the THz pulse (**Figure 2(a)**). A Fourier transform is then used to convert this time domain electrical signal to a frequency domain spectrum (**Figure 2(b)**). The optical path from THz generation to THz detection is purged with dry nitrogen gas to avoid the effect of the humidity.

Dielectric relaxation measurement is a sound method to investigate intermolecular interactions and is capable of monitoring cooperative processes at the molecular level [78–80]. This method is appropriate to monitor molecular motions in widely varied time scales and has been used extensively to study the structure, dynamics, and macroscopic behavior of complex systems [81]. A brief

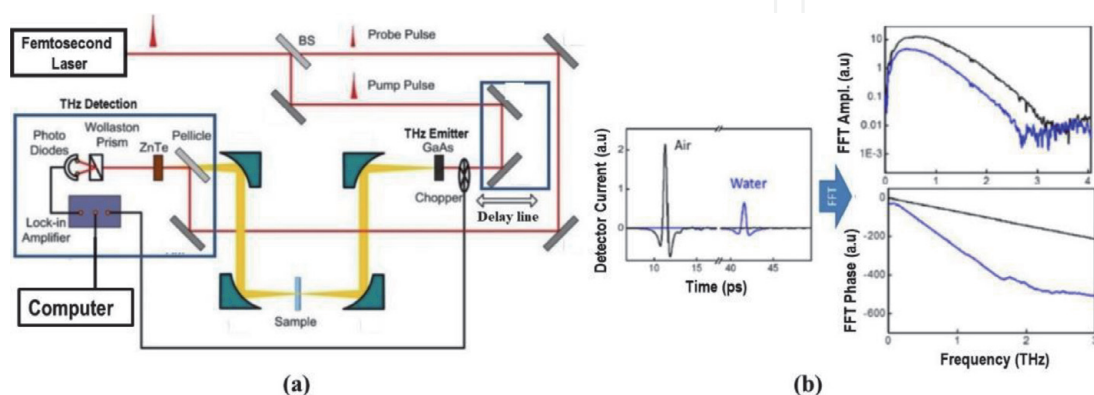


**Figure 2.**

(a): Schematic diagram of a typical THz - time-domain spectrometer. (b): Temporal variation of electric field of the THz pulse and its Fourier transform in air and in presence of water.

discussion (more details may be found elsewhere [81]) on the basic principle of dielectric polarization is presented below.

*Dielectric polarization in static electric field:* If a dielectric material is placed in an external static electric field  $\vec{E}$ , there occurs a charge displacement, which in turn creates a *macroscopic dipole moment* ( $\vec{M}$ ) and this process is known as polarization ( $\vec{P}$ ) or dipole density (**Figure 3**). This polarization is related to the  $\langle \vec{M} \rangle$  (ensemble average) and volume ( $V$ ) of the sample by the following equation,

$$\vec{P} = \frac{\langle \vec{M} \rangle}{V} \quad (7)$$

If a static electric field of strength,  $\vec{E}$ , is applied to an isotropic and uniform dielectric material of dielectric susceptibility  $\chi$ , then the macroscopic polarization can be expressed as,

$$\vec{P} = \epsilon_0 \chi \vec{E} \quad (8)$$

where  $\epsilon_0$  is the dielectric permittivity of the vacuum. Applying the macroscopic Maxwell theory, the electric displacement (electric induction) vector,  $\vec{D}$  can be written as

$$\vec{D} = \epsilon_0 \vec{E} + \vec{P} = \epsilon_0 (1 + \chi) \vec{E} \quad (9)$$

Now, in the linear regime, the relative dielectric permittivity (or *dielectric constant*) is independent of the field strength,  $\epsilon = 1 + \chi$ . Therefore,

$$\vec{D} = \epsilon_0 \epsilon \vec{E} \quad (10)$$

There are different types of polarization mechanisms by an applied electric field in different frequency regions: i) *Ionic polarization*, ii) *Orientation or dipolar rotation polarization*, iii) *Deformation (Atomic and Electronic) polarization*. The total polarization ( $\vec{P}$ ) is the sum of *induced polarization* ( $\vec{P}_\alpha$ ) and *dipole polarization* ( $\vec{P}_\mu$ ).

Therefore,

$$\vec{P}_\alpha + \vec{P}_\mu = \epsilon_0 (\epsilon - 1) \vec{E} \quad (11)$$

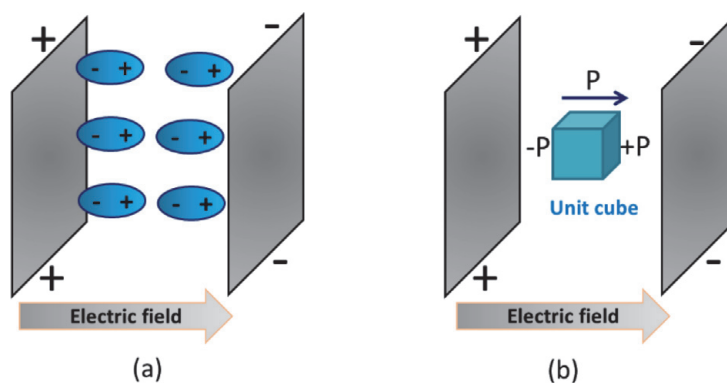


**Figure 3.**  
 (a) Polarization of dielectric. (b) Polarization vector.

For *polar dielectric*, the individual molecule possesses a permanent dipole moment even in the absence of any external electric field but for the *nonpolar* one, there is no dipole moment unless an electric field is applied. Due to the long range of the dipolar forces, an accurate calculation of the interaction of a particular dipole with all other dipoles of a specimen would be very complicated. However, a good approximation can be made by considering that the dipoles beyond a certain distance can be replaced by a continuous medium having the macroscopic dielectric properties. Assuming a continuum with dielectric constant  $\epsilon_\infty$ , in which point dipoles with a moment,  $\mu_d$ , are embedded, we can write the induced polarization as follows,

$$\vec{P}_\alpha = \epsilon_0(\epsilon_\infty - 1)\vec{E} \quad (12)$$

The orientation polarization is given by the dipole density due to the dipoles  $\vec{\mu}_d$ . If we consider a sphere with volume  $V$  comprised of dipoles, we can write,

$$\vec{P}_\mu = \frac{\langle \vec{M}_d \rangle}{V} = \frac{\sum_i (\vec{\mu}_d)_i}{V} \quad (13)$$

*Dielectric polarization in time-dependent electric field:* When a time-dependent electric field is applied, the decay function of dielectric polarization is given by,

$$\phi(t) = \frac{\vec{P}(t)}{\vec{P}(0)} \quad (14)$$

where  $\vec{P}(t)$  is the time-dependent polarization vector. Time-dependent displacement vector  $\vec{D}(t)$  can be written as follows,

$$\vec{D}(t) = \epsilon_0 \vec{E}(t) + \vec{P}(t) \quad (15)$$

$$\vec{D}(t) = \epsilon_0 \left[ \epsilon_\infty \vec{E}(t) + \int_{-\infty}^t \Phi(t') \vec{E}(t-t') dt' \right] \quad (16)$$

where  $\Phi(t)$  is the dielectric response function,  $\Phi(t) = (\epsilon_s - \epsilon_\infty)/[1 - \varphi(t)]$ .  $\epsilon_s$  and  $\epsilon_\infty$  are the dielectric permittivity at low and high frequency, respectively. The frequency dependent complex permittivity  $\epsilon^*(\omega)$  is connected to the above relaxation function through Laplace transformation [82–84],

$$\frac{\epsilon^*(\omega) - \epsilon_\infty}{\epsilon_s - \epsilon_\infty} = \hat{L} \left[ -\frac{d}{dt} \varphi(t) \right] \quad (17)$$

where  $\hat{L}$  is the operator of the Laplace transformation, which is defined for the arbitrary time dependent function  $f(t)$  as,

$$\hat{L}[f(t)] \equiv F(\omega) = \int_0^\infty e^{-pt} f(t) dt \quad (18)$$

where  $p = x + i\omega$  and  $x \rightarrow 0$ .

Eq. (17) gives equivalent information on dielectric relaxation properties of the sample both in frequency domain and time domain measurements. Therefore, the

dielectric response might be measured experimentally as a function of either frequency or time, providing data in the form of a dielectric spectrum  $\epsilon^*(\omega)$  or the macroscopic relaxation function  $\varphi(t)$ . For instance, when a macroscopic relaxation function obeys the simple exponential law,

$$\varphi(t) = \exp\left(-\frac{t}{\tau_m}\right) \quad (19)$$

Where,  $\tau_m$  indicates the relaxation time. Eqs. (17) and (19) give rise to the following relation,

$$\frac{\epsilon^*(\omega) - \epsilon_\infty}{\epsilon_s - \epsilon_\infty} = \frac{1}{1 + i\omega\tau_m} \quad (20)$$

i.e,

$$\epsilon^*(\omega) = \epsilon_\infty + \frac{\epsilon_s - \epsilon_\infty}{1 + i\omega\tau_m} \quad (21)$$

This is known as the Debye model for frequency dependent dielectric permittivity. According to the Debye model, the complex frequency dependent dielectric response [ $\tilde{\epsilon}(\nu) = \epsilon_{real}(\nu) - i\epsilon_{imaginary}(\nu)$ ] can be described as:

$$\tilde{\epsilon}(\nu) = \epsilon_\infty + \sum_{j=1}^m \frac{\epsilon_j - \epsilon_{j+1}}{1 + i2\pi\nu\tau_j} + \frac{\sigma}{i2\pi\nu\epsilon_0} \quad (22)$$

where,  $\epsilon_0$  is the permittivity in free space ( $= 8.854 \times 10^{-12}$  F/m),  $\omega = 2\pi\nu$  is the angular frequency,  $\tau_j$  is the relaxation time for the  $j$ -th relaxation mode,  $\epsilon_1$  is the static dielectric constant,  $\epsilon_j$  are the dielectric constants for different relaxation processes,  $\epsilon_\infty$  is the extrapolated dielectric constant at a very high frequency and  $m$  describes the number of relaxation modes.

### 3. Structure and dynamics of hydration layer in interfaces of small molecules, proteins, peptides, nucleic acids and membranes

The dynamics of water around small as well as complex molecules changes owing to their specific interaction with the solute surface; the specific nature of the interaction could mostly be electrostatic or hydrogen bonding. Such interaction expectedly ruptures/modifies the tetrahedral water network structure as well as its dynamics, a clear imprint of that gets reflected in the THz frequency window. Measurement of optical parameters  $\alpha(\nu)$  and  $n(\nu)$  enables one to determine the change in water dynamics at the vicinity of (bio)surface and consequently one can infer on the changes of the corresponding solute also.

#### 3.1 Ions

Metal ions are perhaps the simplest solutes that can induce perturbation in water dynamics, the interaction being mostly electrostatic in nature. A systematic investigation using alkali monovalent cations [85] and alkaline earth bivalent cations [86] in aqueous solutions have been put forward by the group of Martina Havenith using far-IR and THz FTIR measurements coupled with classical MD simulation studies.

Their study concluded that ion rattling motions can account for the observed changes in the THz absorption. They have shown that the spectrum of the salt solutions can be approximated by a linear superposition of concentration weighted neat water and ion contributions. Ab initio MD simulation study by Marx et al. [87] has successfully reproduced the spectral responses of the solvation shell around the ions in infrared and THz frequency range. Their study has shown that the solute-solvent dipolar couplings and the dipole-dipole correlations are the important factors that govern the absorption features in this frequency regions. The group of Martina Havenith has subsequently put forward a series of studies on the hydration dynamics of heavy metal ions, e.g. lithium [88], manganese [89], iron [90] and ytterbium [91]. An elaborate description of the process involved has recently been put forward by this group [92]. The overall THz effect of the ions could be apprehended in terms of the contributions from various modes as depicted in **Figure 4**.

In a systematic study using THz-TDS in the frequency region (0.3–2.1 THz;  $10\text{--}70\text{ cm}^{-1}$ ), experimental evidences for the ultrafast collective hydrogen bond dynamics of water in the extended hydration layers of alkali metal chlorides have been obtained [93]. The real and imaginary part of the permittivity ( $\epsilon$ ), as obtained from the THz-TDS measurements was fitted using a triple Debye relaxation model. The time scales obtained for bulk water are of the order of  $\sim 8\text{--}9\text{ ps}$  ( $\tau_1$ ),  $200\text{ fs}$  ( $\tau_2$ ) and  $80\text{ fs}$  ( $\tau_3$ ). The  $\sim 9\text{ ps}$  and  $\sim 200\text{ fs}$  timescales are due to the well-known cooperative rearrangement of the H-bonded network structure and the small angular rotational modes of individual polar water molecules, respectively. It has been reported that ( $\tau_1$ ) decreases with increasing salt concentration, which identifies an acceleration of the cooperative hydrogen bond dynamics affirming a positive support towards the most debated notion of these ions to act as water structure breakers (see **Figure 5(a)**). The extent of this effect has been found to be mostly ion specific,  $\text{K}^+$  being the most effective ion and a simple consideration of ionic charge density is insufficient to account for the observed changes. Very recently, Havenith and Marx [94] have put forward a combined experimental and simulation investigation to provide a detailed mechanistic analyses based on cross-correlation analysis (CCA) technique to understand the minute details of water-solute interactions.

### 3.2 Complex ions and small molecules

While the interaction of metal ions with water is more straight-forward, complexity arises when an ion is associated with a hydrophobic moiety. Such molecules

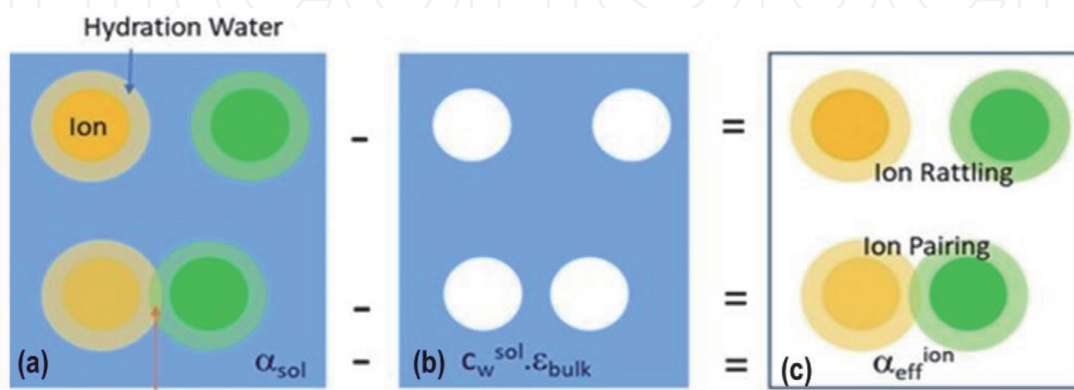


**Figure 4.** Schematic representation of ion hydration. (a): Bulk-like water (blue), water around ions (yellow and green), and hydration water (lighter shades of yellow and green). The total absorption of the solution ( $\alpha_{sol}$ ) has contribution from all. (b): Concentration-weighted bulk-water values are subtracted from  $\alpha_{sol}$ . (c): This yields the effective absorption of the solvated ion or ion pair ( $\alpha_{eff}^{ion}$ ).

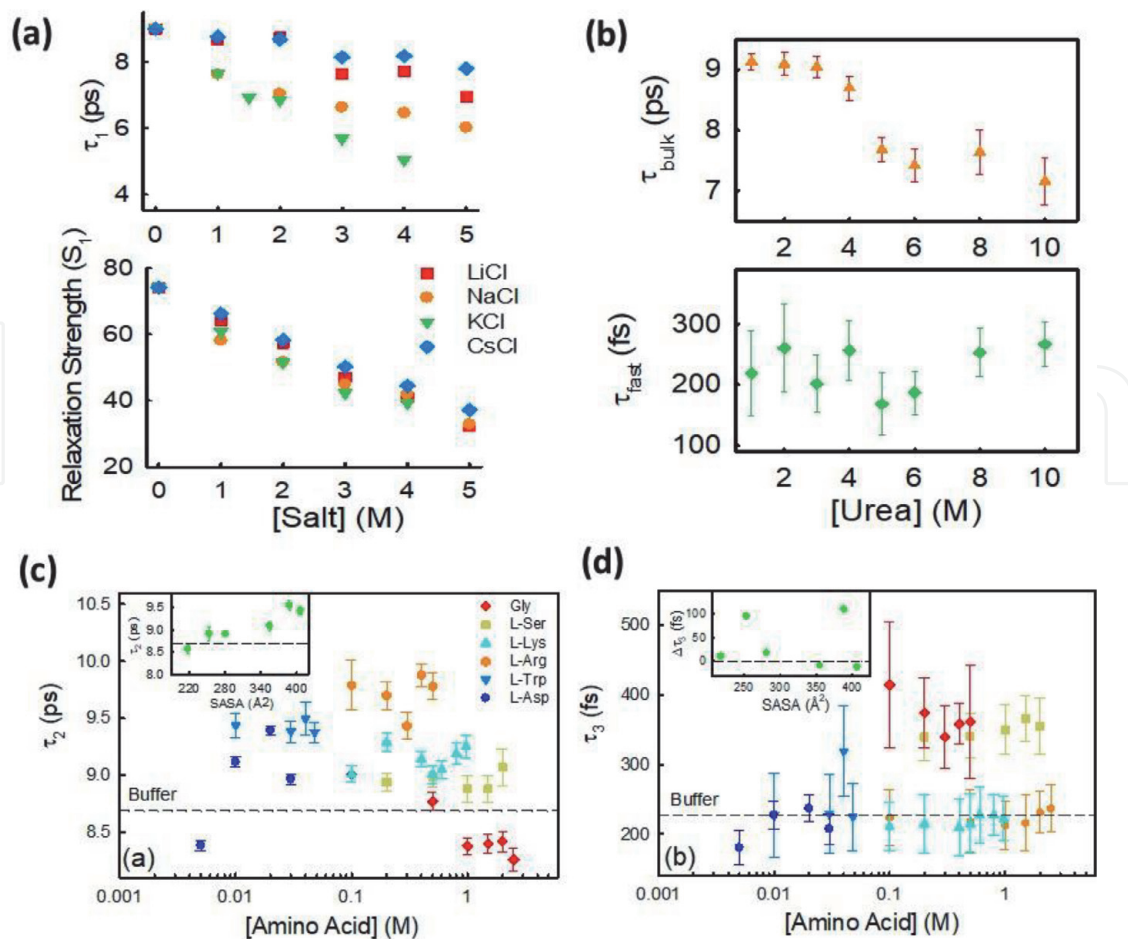


**Figure 5.** (a) Cooperative relaxation dynamics ( $\tau_1$ ) and relaxation strength ( $S_1$ ) of aqueous solutions of different alkaline metal cations. (b) Relaxation dynamics (as defined by the timescales  $\tau_1$  and  $\tau_2$  of aqueous urea solution as a function of urea concentration. A sharp change in the  $\tau_1$  is observed at  $\sim 4$  M urea. (c) Cooperative hydrogen bond relaxation time constant ( $\tau_2$ ) of aqueous solutions of amino acids as a function of their concentration. The dotted line is the time constant for the buffer solution. The inset shows the change in  $\tau_2$  (measured at maximum amino acid concentration) as a function of the SASA of amino acid. (d) Relaxation time scale  $\tau_3$  corresponding to the jump orientation of water (obtained by Debye fitting of THz data) of different amino acids solutions. The dotted line is the time constant for that of the buffer. The inset shows the change in the timescale ( $\Delta\tau_3 = \tau_{\text{solution}} - \tau_{\text{buffer}}$ ) at the maximum concentration of the amino acids.

are often of biological importance and therefore their interaction with water is essential to establish. There have been several reports on the THz studies of sucrose and saccharides [95–99]. In a pioneering work Heyden et al. [100] have described the nature of hydration around small carbohydrate molecules and a detailed simulation study has revealed that the extent of the hydration shell and their absorption co-efficient change with the solute specificity. One such molecule is urea, which is well known to be a protein denaturant, however, the exact molecular mechanism of the processes involved still remains a strongly debatable issue, specially the argument of whether the interaction is water mediated (the water structure breakers notion of urea) or a direct interaction of urea with protein surface.

An elaborate attempt has been made to understand the effect of urea (and its derivatives) on the ultrafast solvation dynamics of water using a Debye type dielectric relaxation model in the 0.3–2.0 THz frequency region using THz-TDS technique [101]. The relaxation dynamics shows considerable acceleration beyond a threshold concentration. Such acceleration is possibly associated with a disruption of the tetrahedral water network structure. It seems also intriguing that the observed collapse occurs at a certain urea concentration (see **Figure 5(b)**), which strikingly coincides with the denaturation concentration of urea for many proteins.

Another molecule of such biological interest is guanidinium chloride (GdmCl), which offers remarkable protein denaturation ability beyond a certain threshold concentration ( $\sim 2\text{--}3\text{ M}$ ) [102, 103]. Like in the case of urea, protein denaturation mechanism of GdmCl has also been debatable concerning a direct or indirect interaction. We have investigated the collective hydrogen bond dynamics around GdmCl in aqueous solutions as well as in the presence of a model globular protein human serum albumin (HSA) using the THz-TDS technique. It is found that the relaxation dynamics gets faster which renders support to the previously speculated notion that GdmCl acts as a water structure breaker. A similar but more prominent trend is observed in case of NaCl, which, however, does not interact with proteins.

The change in hydration dynamics in presence of HSA has been found to be in complete contrast in these two salts unambiguously pointing out towards a possibility of the collective hydration dynamics to share a pivotal contribution in the protein unfolding phenomenon. These studies seem to conjecture that ions with complex hydrophobic moiety acts as water structure breaker, and this very nature of such molecules makes them protein denaturant. To investigate the validity of such conjecture we investigated the ultrafast (sub-ps to ps) collective hydrogen bond dynamics of water in the extended hydration layers in a series of alkylammonium chloride salts using THz-TDS technique [104]. We found these salts to transform from being a water 'structure breaker' to 'structure maker' with increasing carbon content. For example, the THz-TDS measurements reveal that ammonium chloride (AC) acts as a water network structure breaker while tri-ethyl ammonium chloride (EAC) and higher carbon containing salts are distinct water structure makers. The change in protein hydration is also found to trace its secondary structure rupture and the exposure of hydrophobic moieties accordingly changes the protein hydration. Our study strongly concludes that it is the hydrophobic effect, at least in the case of this type of salts, that plays the decisive role in determining their interaction with biomolecules.

### 3.3 Amino acids

Amino acids, which are the building blocks of proteins, often act as intermediates in metabolism as well as osmolytes that can stabilize proteins. Depending upon the 'side group', the amino acids are classified as hydrophilic or hydrophobic. Hydrophobicity of amino acids is believed to be a key parameter that regulates phenomena like protein folding - unfolding, aggregation, activity, protein-ligand binding and protein hydration in aqueous environments. While to analyze the solvation of hydrophobic and hydrophilic parts of a protein separately, one needs to take into consideration that the environment of amino acid residues is heterogeneous in nature as they are often composed of hydrophobic alkyl chains and hydrophilic groups. It is therefore essential to study the hydration of amino acids of various side chains in the exposure to solvents. Niehues et al. [105] have studied the hydration of a series of amino acids in  $\sim 2.4\text{ THz}$  window and observed that the THz absorption coefficient,  $\alpha(\nu_{\text{THz}})$ , of hydrated amino acids can be correlated with the hydrophobicity and the fraction of polar volume of amino acids. They have shown that glycine has the largest positive THz slope followed by serine, whereas for the other amino acids, the slope becomes gradually negative with increasing hydrophobicity. In another study [106], the same group, by analyzing the corresponding THz spectrum in terms of the correlated dynamics of solute and solvent molecules, demonstrates the line shape of the low-frequency vibrational response of glycine in water. Recently, they [107] have shown that hydrophilic solvation of the zwitterionic groups in valine and glycine leads to similar THz responses, which are fully decoupled from the side chain. This result concludes that the hydrophilic groups

and their solvation shells dominate the THz absorption difference, while on the same intensity scale, the influence of hydrophobic water can be neglected. Shiraga et al. [108] concludes a correlation between the extent of H-bonding and the hydrophobicity of the solute. Glycine (Gly) and the L- isomers of five different amino acids: serine (Ser), aspartic acid (Asp), lysine (Lys), arginine (Arg) and tryptophan (Trp) of varying hydrophobicity and solvent accessible surface area (SASA) have been used by Samanta et al. [109] to study the dielectric relaxation up to their maximum water solubility in the frequency window of GHz-THz at neutral pH. The various rotational dynamics of the solutes and water are obtained by fitting the dielectric data in a multiple Debye relaxation model. From GHz study, we observed that the molecular rotation of amino acids correlates their respective molecular volume. Also, it was concluded that the amino acids do not usually aggregate even at high concentrations. From THz study, the authors found that Gly is a water structure breaker while the other amino acids are structure makers. Consequently, Gly accelerates cooperative hydration, while the others retard (see **Figure 5(c)** and **(d)**). It has been established that hydration in amino acids depends both on its hydrophobic as well as its hydrophilic nature of side chains. Born et al. [110] have studied the hydration dynamics of some small model peptides using THz spectroscopy. They observed that the cooperative hydration dynamics changes as the extent of hydration of such molecules change.

### 3.4 Alcohols and other solvents

Addition of otherwise indifferent organic solvents can influence marked changes in aqueous environments as well as they can induce malfunction in biologically important molecules e.g. protein, DNA, etc. Water - dimethyl sulfoxide (DMSO) binary mixture has been found to be of potential interest as it plays a significant role in the field of chemistry, physics, biology and pharmacology. Das Mahanta et al. have investigated the change in the collective hydration dynamics in presence of DMSO at different concentrations using THz-TDS. We found that  $\alpha(\nu)$  of the mixed solvents shows a non-linear change with  $X_{\text{DMSO}}$  [111]. This change has been correlated with the water-DMSO structural heterogeneity in the mixed solvents. Luong et al. have also studied the evolution of water hydrogen bonded collective network dynamics in water - 1,4-dioxane (Dx) mixtures as the mole fraction of water ( $X_w$ ) increases from 0.005 to 0.54 [112]. The inter- and intra-molecular vibrations of water be observed using THz-TDS in the frequency range 0.4–1.4 THz (13–47  $\text{cm}^{-1}$ ) and Fourier transform infrared (FTIR) spectroscopy in the far-infrared (30–650  $\text{cm}^{-1}$ ) regions. From the absorption coefficient measurements, they infer that the mixtures are not ideal in nature, which suggests a significant change in the network by the addition of the solute. The authors found an increase in the collective hydrogen bond network as evidenced from dielectric relaxation studies in which  $\tau_1$  has been found to be small at low  $X_w$  (where  $X_w$  is the mole fraction of water in the mixture), but at  $X_w > 0.1$ , it increases rapidly to reach a value identical to that in bulk water. It has been concluded that hetero-molecular (water - Dx) hydrogen bond dominates in the water diluted region in water-Dx mixtures, and with progressive addition of water, bulk-like intermolecular three-dimensional hydrogen bonded water network dynamics evolves beyond  $X_w = 0.1$ . In a separate study [113], a combined experimental (mid- and far-infrared FTIR spectroscopy, THz-TDS (0.3–1.6 THz)) and molecular dynamics (MD) simulation technique has been carried out to understand the evolution of the structure and dynamics of water in its binary mixture with 1,2-dimethoxy ethane (DME) over the entire concentration range. Debye relaxation data reveals a non-monotonous behavior in which the collective dynamics is much faster in the low  $X_w$  region, whereas in the  $X_w \sim 0.8$

region, the dynamics gets slower than that of pure water. The concentration dependence of the reorientation times of water, estimated from the MD simulations, also captures this non-monotonous character. Bohm et al. [114] have demonstrated that the THz response of alcohols can be decomposed into the spectrum of bulk water, tetrahedral hydration water, and more disordered (or interstitial) hydration water. They also concluded that it is not the tetrahedrally ordered component, rather it is the interstitial hydration water which is responsible for the temperature-dependent change in  $\Delta C_p$  and  $\Delta G$  in such mixtures.

### 3.5 Proteins

The surface of proteins is extremely heterogeneous owing to the presence of amino acids of varying types of charges. The pioneering studies by the group of Havenith et al. have shown that protein molecules are hydrated and the cooperative dynamics of water changes accordingly. An earlier study using a small protein ubiquitin [115] shows how the measurement of  $\alpha(\nu_{\text{THz}})$  reveals a change in the protein hydration dynamics as the authors termed it as the “THz dance”. In a subsequent ever important simulation paper, the same group has established different THz absorption of the hydrophobic and hydrophilic residues of a protein as they interact differently with water [116]. In the later years, this group has put forward substantial contribution on the hydration dynamics of proteins using THz measurements [117, 118] as well as simulation studies [42, 119]. Their studies have unambiguously suggested that fast protein motion and solvent dynamics are correlated with enzymatic reactions [120]. In a recent study this group has established the pivotal role of collective motion of water during an electron transfer reaction between flavoenzyme ferredoxin - NADP<sup>+</sup> – reductase and ferredoxin-1 [121]. In a seminal paper, Marklez et al. [122] have used THz-TDS measurements to show that the protein (hen egg white lysozyme) dynamical transition (the rapid increase in protein dynamics occurring at  $\sim 200$  K) needs neither tertiary nor secondary structure. Their results revealed that the temperature dependency essentially arises from the protein side-chain interaction with the solvent. He et al. [123] have investigated the presence of structural collective motions on a picosecond timescale for the heme protein, cytochrome C, as a function of oxidation and hydration, using THz-TDS and molecular dynamics simulations. Marklez group has developed a novel measurement technique (anisotropy THz microscopy) [124] wherein they were able to detect the long range protein vibration modes in chicken egg white lysozyme single crystals. They found the underdamped modes to exist for frequencies  $>10\text{ cm}^{-1}$ . Such underdamped vibrational modes have also been identified using optical Kerr effect measurements in the THz frequency window [125]. In a recent study, Niessen et al. [126] have used anisotropy THz microscopy, which is found to be sensitive to inhibitor binding and unique vibrational spectra for several proteins and an RNA G-quadruplex. There have been other reports from several experimental groups: Sun et al. [127] have reported the application of a new machine learning methods for quantitative characterization of bovine serum albumin (BSA) deposited thin-films detected by THz-TDS. The group of Emma Pickwell-MacPherson [128] have used THz spectroscopy to study the hydration shell formation around H9 subtype influenza A virus’s HA protein (H9 HA). They have also detected antigen binding of H9 HA with the broadly neutralizing monoclonal antibody. They observed a remarkable concentration dependent nonlinear response of the H9 HA, which reveals the formation process of the hydration shell around H9 HA molecules. The same group has also reported the dielectric properties of two different antibodies in water-glycerol mixtures using THz-TDS measurements [129]. Sun et al. [130] used THz-TDS to investigate the molecular processes involved above and below the transition temperature ( $T_D$ ) for GP2 peptide.

### 3.6 DNA

While much research has been focused on proteins, relatively less attention has been paid on the other biologically important molecule, DNA. There had been a few preliminary studies to understand the vibronic bands in the THz frequency region using single and double stranded DNAs and RNAs [131–133]. Arora et al. [134] have presented a label free quantitative detection method for DNA samples amplified by polymerase chain reaction (PCR) in aqueous medium using THz-TDS in the frequency range from 0.3 to 1.2 THz. Tang et al. [135] have recently investigated the feasibility of THz spectroscopy combined with microstructures for marker-free detection of DNA and oligonucleotides. Polley et al. have investigated the collective dynamics of two DNA molecules extracted from salmon sperm and calf thymus and observed that the dynamics did not differ much at the concentration range of the experiments [136].

### 3.7 Lipid membrane

There have been only limited studies on the THz studies on lipid membranes and/or vesicles. One of the preliminary results was due to Tielrooij et al. [137] who had studied the dielectric relaxation in mixed system of hydrated DOPC lipid bilayers in the THz frequency domain. They could identify three distinct water types: fast, bulk and irrotational. The relative content of those change with the extent of hydration. Later, Yamamoto et al. [138] have studied the temperature and hydration dependent low frequency spectra of lipid bilayers of 1,2-dimyristoyl-sn-glycero-3-phosphoryl-3'-rac-glycerol (DMPG) and 1,2-dimyristoyl-sn-glycero-3-phosphocholine (DMPC) using THz-TDS. They found that the THz absorption patterns reflect the lipid packing pattern in the bilayers. They subsequently extended their investigations towards purple membrane (PM, a complex of lipids and a membrane protein, bacteriorhodopsin) [139] and lipid bilayer of DMPC [140]. Pal et al. have recently studied the microstructure and collective dynamics of the membrane interfacial hydration shell in zwitterionic and negatively charged phospholipid membrane bilayers using THz-TDS [141]. They observed a dependence of the critical lipid concentration corresponding to the inflection point on the charge of the lipid head-group, thereby implicating membrane electrostatics as a major factor in the microstructure and dynamics of water at the membrane interface.

## 4. Influence of temperature, pH, ionic strength and additives on hydration layer dynamics

Hydration dynamics of biomolecules is significantly influenced upon changing its physical conditions as well as in the presence of additional chemical agents, like alcohols, glycols, etc. Protein molecules undergo various physical and chemical changes, which could induce conformational modifications in their secondary as well as tertiary structures. It can be noted here that as protein structures get disrupted (during unfolding or denaturation) the hydrophobic moieties (amino acid residues), which are otherwise buried inside in the native structure, get exposed, and this produces a definite alteration in THz absorption coefficient,  $\alpha(\nu_{\text{THz}})$ . It therefore suggests that estimation of  $\alpha(\nu_{\text{THz}})$  provides a direct evidence of the structural perturbation in proteins.

Several experimental techniques are available to determine the structural evolution of proteins during unfolding, while THz provides with the estimation of the associated hydration changes. In a pioneering experimental work, in which a

stopped-flow techniques was synchronized with THz-TDS, which the authors termed as Kinetic terahertz absorption (KITA) spectroscopy, Kim et al. [142] have shown that the pH induced unfolding-refolding kinetics (in real time) of Ub\* could easily be traced by the associated  $\alpha(\nu_{\text{THz}})$  measurements. The THz results very well reconcile with the results obtained from circular dichroism (CD) and fluorescence measurements.

Another important physical environment that induces protein unfolding is temperature. In a study using HSA as a model protein, Mitra and Havenith [143] have shown that water dynamics associated with the protein during its reversible unfolding pathway up to 55°C as well as its irreversible denaturation pathway up to 70°C traces the protein's structural rupture pathway. The THz measurements do support the conventional CD and fluorescence measurements. Sudden increase in the environment (like temperature or pressure) for a very short period of time (often termed as T-jump experiments) leads protein molecules to be structurally ruptured but upon removal of the intense pulse, the protein refolds. T-jump experiments have previously been characterized using conventional CD and fluorescence measurements. However, THz measurements was demanded to obtain explicit information of water dynamics. The first report of such experiment was from the group of Havenith [144], wherein the authors put forward a coupled KITA setup with a T-jump attachment. The authors monitored changes in the THz absorption  $\lambda^{*6-85}$  protein with a time resolution of  $>50 \mu\text{s}$ . They reported that the spectral changes are correlated with the hydrophobic collapse of the protein. In a subsequent study from the same group, Wirtz et al. [145] used an even better time resolution of about 500 ns to reveal the coupled ubiquitin–solvent dynamics in the initial phase of hydrophobic collapse (temperature induced unfolding). They propose that, in the case of ubiquitin, a rapid ( $\sim 500$  ns) initial phase of the hydrophobic collapse from the elongated protein to a molten globule structure precedes secondary structure formation. Recently there have been a few reports of using THz spectroscopy technique to underline thermal denaturation of BSA [146], temperature- and pH-dependent protein conformational changes in pepsin A [147]. In a very recent study Cao et al. [148] have successfully employed THz-TDS to track the hydrolysis of BSA protein by pepsin. The results indicate that protein hydrolysis can be easily monitored over time by focusing on the variation of the absorption coefficient from a macroscopic perspective. The authors explored the use of the Debye model to analyze the dielectric properties of the solution during protein hydrolysis. The results of the Debye analysis prove that it is possible to investigate in detail the microscopic dynamics of bio-macromolecule solutions at the molecular level by THz-TDS.

Samanta et al. have been involved in determining the changes in protein hydration in various distressed environments using the THz-TDS measurements. They have investigated the hydration dynamics around HSA in presence of short chain polyethylene glycols of different chain lengths (PEG 200, PEG 400, and PEG 10000) at different concentrations [149]. FIR-FTIR studies conclude that the protein hydration is affected in a distinct way below and above the critical PEG concentration of 30% (v/v). THz-TDS study unambiguously confirmed a retardation of the solvation dynamics by PEGs. This study clearly shows an independent behavior of protein hydration at low PEG concentrations and a noticeable interaction between protein and PEG hydration beyond a critical PEG concentration. In another study, Das et al. have made an attempt to understand whether the DMSO induced conformation changes in lysozyme conformation perturbs its hydration dynamics [150]. CD study establishes a marked change in the protein tertiary structure in presence of DMSO. The relative change in the THz absorption coefficient ( $\Delta\alpha/\alpha_0$ ) shows a negative minimum at  $X_{\text{DMSO}} = 0.05$  and a positive value at

$X_{\text{DMSO}} = 0.15$ . The observed minimum is found to be due to the increased size of the protein while the positive value is attributed to the increased SASA and consequent increased hydration of the protein surface. In a recent report, Das et al. put forward an experimental observation of nonmonotonic changes in the collective hydration of BSA in the presence of alcohols of varying carbon-chain lengths, that is, ethanol, 2-propanol, and tert-butyl alcohol (TBA), by using THz – TDS [151]. They observe an anomalous hydration behavior of the protein hydration with the alcohol concentration, which correlates the alcohol-induced  $\alpha$ -helix to random coil transition of the protein secondary structure, as revealed by CD spectroscopy measurements. Recently, Das Mahanta have investigated the effect of alkyl-ammonium chloride salts on BSA and found a systematic trend towards disrupting the protein secondary structure [104]. The associated changes in the protein hydration in the presence of these salts have also been investigated using THz-TDS. The change in protein hydration is also found to trace its secondary structure rupture, and the exposure of hydrophobic moieties accordingly change the protein hydration. The THz-TDS measurements strongly conclude that it is the hydrophobic effect, at least in the case of this type of salts, that plays the decisive role in determining their interaction with biomolecules.

## **5. Role of hydration water in protein aggregation and fibrillation**

Aggregated protein is toxic to functioning of living systems and many of human diseases are associated with misfolded protein disorders [152–156]. This is why understanding of mechanisms of interactions between protein molecules in solutions have been the subject of extensive investigations during the last two decades [157–161]. Additionally, understanding the protein aggregation propensity may offer novel design principles for producing aggregation-resistant proteins for biotherapeutics.

Globular proteins, e.g. HSA and BSA, in their native states are present in living cells at concentrations as high as about  $200 \text{ mg mL}^{-1}$  and bimolecular interactions are significant. We explained earlier that stability of the three - dimensional structure of a monomeric protein molecule in physiological environments is the result of an intricate interplay between electrostatic, hydrophobic, hydrogen bonding and other interactions and any variation of temperature, pH of the medium or any other physiochemical conditions including concentration of protein in the cell may result in imbalance of the stabilization forces leading to misfolding [162, 163], thus triggering aggregation [164–168].

A native and structurally stable protein molecule is strongly hydrated with a well-defined hydration layer of thickness of about a few tens of Å (20–40 Å) around it [50, 59, 169]. The role of water molecules in the hydration shell could be crucial for the intermolecular interactions and the overall protein hydrophobicity, which may be defined by its hydration free energy, which may play an important role in protein aggregation in aqueous solution [162, 163, 166]. However, the role of hydration water in protein aggregation has largely been unexplored owing to the perception that protein – protein interaction is the major factor and the surrounding water is just a spectator playing no role in aggregation of protein, ignoring water as an active constituent of biological systems. In fact, whether a protein remains soluble or forms aggregation should intrinsically rely on its state of hydration in the monomeric state.

We have described in the earlier sections of this article that how the properties of water molecules in the hydration layer on an average are different from those in the bulk, which determines the stability of a monomer protein in aqueous

environment. Protein aggregation proceeds through a multistep process initiated by conformational transitions, called protein misfolding, of monomer species towards aggregation-prone structures. Chong and Ham applied the fluctuating thermodynamic analysis method to understand the variations of the thermodynamic functions, which occur during the course of misfolding and dimerization of the Amylase- $\beta$  protein. They suggest that the time variation of the solvent-averaged effective energy,  $F = E_u + G_{\text{solv}}$ , describes the protein dynamics on the free energy landscape [170]. Here, the protein potential energy ( $E_u$ ), comprises both intra and intermonomer contributions and the solvation free energy ( $G_{\text{solv}}$ ), represents the interaction of the protein with surrounding water, which plays a critical role in protein aggregation. The free energy,  $F$ , decreases as the dimerization proceeds, but the decrease in  $F$  has different origins in the approach and structural adjustment regimes. The thermodynamic force driving the approach of two monomers is the decrease in  $G_{\text{solv}}$  and hence, the misfolded monomers acquire a large hydrophobicity, which leads to conformational changes in monomers. This drives two monomers to approach each other to a contact distance. In absence of this thermodynamic driving forces, two negatively charged protein monomers (the total charge of Amylase- $\beta$  and BSA monomer proteins at neutral pH are  $-3$ , and  $-16$ , respectively [170, 171]) would never approach each other by overcoming the electrostatic repulsion. On the other hand, decrease of the protein potential energy  $E_u$ , due to direct protein-protein interactions, such as intermonomer van der Waals contacts and hydrogen bonds, drives the structural rearrangement required for formation of compact dimer structure leading to energetic stabilization. Interestingly, structural rearrangements are also associated with an increase in the solvation free energy, which originates from the dehydration of the protein surface and of the interfacial region. On contrast to other spectroscopic techniques, THz spectroscopy probes directly the collective intermolecular vibrations of the hydrogen bond network, and is thus able to detect sensitively solute induced changes in the solvation dynamics. Extensive works on THz absorption of protein solutions have demonstrated that the absorption coefficient of the protein solutions ( $\alpha_{\text{sol}}$ ) are dependent on the concentration of protein [50, 59, 169–171]. For example, at the low concentration regime (e.g. in the case of HSA,  $< 0.5 \times 10^{-3} \text{ mol dm}^{-3}$ )  $\alpha_{\text{sol}}$  value increases linearly and this has been explained by increasing concentration of hydrated monomer protein molecules since water in the hydration shell has larger  $\alpha_{\text{sol}}$  value as compared to that of bulk water. However, on further increase of the protein concentration,  $\alpha_{\text{sol}}$  value starts decreasing.

To delineate this issue in more detail, Manna et al. made a detailed investigation on the concentration dependence of THz absorption of the aqueous buffered solutions of HSA protein (up to 2.6 mM of protein concentration) at three THz frequencies, namely, 0.1, 1.5 and 2 THz [59]. Similar results were obtained from these three measurements.  $\alpha_{\text{sol}}$  value was expected to change linearly to follow Eqs. (23) and (24), which could be derived assuming that the protein solution is a two-component system.

$$\alpha_{\text{sol}} = \alpha_{\text{pr}} V_{\text{pr}} + \alpha_{\text{bw}} V_{\text{bw}} \quad (23)$$

$$\left( \frac{\alpha_{\text{sol}}}{\alpha_{\text{bw}}} \right) = \left( \frac{\alpha_{\text{pr}}}{\alpha_{\text{bw}}} \right) V_{\text{pr}} + V_{\text{bw}} = (1 - 0.08 [\text{HSA}]) \quad (24)$$

Here,  $\alpha_{\text{pr}}$  is the absorption coefficient of the protein,  $\alpha_{\text{bw}}$  is the absorption coefficient of bulk water,  $V_{\text{pr}}$  is the volume fraction occupied by protein molecules and  $V_{\text{bw}}$  is the volume fraction occupied by bulk water. Eq. (24) was derived using several considerations, such as the value of the radius of gyration of HSA is about 3.3 nm [172], the structure of the monomer HSA protein molecule consists of

hydrophobic and hydrophilic pores (2: 1 (v/v) ratio) with porosity factor of about 33% of the volume of the protein molecule [173].

Therefore, the plots of  $\left(\frac{\alpha_{sol}}{\alpha_{bw}}\right)$  against HSA concentration, [HSA], as shown in **Figure 6** (red lines), represent the two-component system. However, a large deviation of the experimental data points from the line representing two component system suggests inadequacy of the two-component model. This deviation could be explained by considering that the THz absorption coefficients of the water molecules in the hydration layer, ( $\alpha_{hl}$ ), were different from that of bulk water ( $\alpha_{bw}$ ) and hence constitute the third component in the aqueous solution of the protein. Hence, Eq. (25), in which  $V_{hl}$  was the total volume fraction of water associated with the protein molecules in a solution with protein concentration of  $1 \times 10^{-3} \text{ mol dm}^{-3}$ , was derived [59].

$$\left(\frac{\alpha_{sol}}{\alpha_{bw}}\right) = \left(\frac{\alpha_{hl} V_{hl}}{\alpha_{bw}}\right) C_{pr} + (1 - 0.08 C_{pr} - V_{hl} C_{pr}) \quad (25)$$

To understand the reasons for significant decrease of THz absorption coefficient of the protein solutions with increasing concentration beyond  $6 \times 10^{-4} \text{ mol dm}^{-3}$ , the possibility of aggregation of proteins at higher concentration regime was explored. To delineate this aspect, dynamic light scattering (DLS) measurements (**Figure 6**) were carried out using concentrations of proteins covering the entire range of THz absorption measurements. The DLS data recorded for the solution containing protein concentration of  $0.4 \times 10^{-3} \text{ mol dm}^{-3}$  revealed the existence of only monomeric protein molecules with the most probable diameter of about 6–8 nm in the solution. This is quite in good agreement with the diameter of the

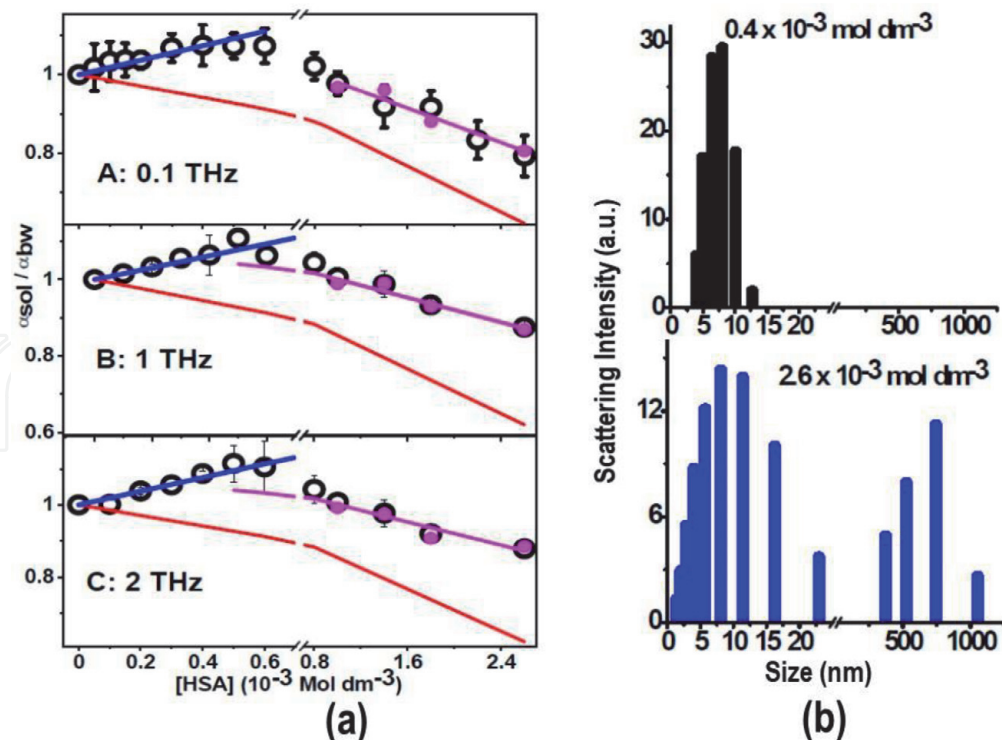


**Figure 6.**

(a): Plots of  $\left(\frac{\alpha_{sol}}{\alpha_{bw}}\right)$  vs. [HSA] recorded at three THz frequencies. Black squares with error bars are the experimental points. Red line represents two component system as per Eq. (24). Best nonlinear fit to the experimental points in the low concentration regime (up to  $6 \times 10^{-4} \text{ Mol dm}^{-3}$ ) using Eq. (25). Violet line is the linear fit to the experimental points at protein concentrations larger than  $8 \times 10^{-4} \text{ Mol dm}^{-3}$  using Eq. (26). (b): Size distribution of particles in solutions of two different CONCENTRATIONS of HSA as obtained from DLS analysis.

hydrated monomer protein molecules. However, at higher concentrations (say,  $>1 \times 10^{-3} \text{ mol dm}^{-3}$  of protein), the DLS data revealed two important features. Firstly, the size distribution of the monomer band became wider indicating the presence of particles of diameter in the range 12–15 nm, possibly suggesting formation of dimers or trimers of HSA, in addition to the monomeric species. Secondly, at higher concentrations of the protein, DLS data also revealed the presence of large size aggregates of the most probable diameter of about 700 nm. However, a quantitative estimation of the relative percentages of monomer, dimer and aggregates was not possible from the DLS data because the intensity distribution of the scattered radiation was not directly proportional to the number of the particles. However, this experiment confirmed the presence of protein aggregates in solutions with higher concentrations of protein and the formation of aggregates may possibly be held responsible for nonlinear dependence of THz.

On the other hand, CD measurements confirmed that the tertiary structure of HSA remained unchanged through the entire range of HSA concentrations used for THz measurements. This suggested that the native structure of HSA molecules remained unaltered through the entire range of concentrations of HSA. Therefore, hydration states of proteins, even in the aggregated state, remain unchanged and hence possibly justifies the assumption made in the earlier works regarding overlapping of hydration shells at higher concentrations of proteins.

Patro and Przybycien have simulated the structures of reversible protein aggregates as a function of protein surface characteristics, protein–protein interaction energies and assessed the aggregate properties [174]. Results of their simulation reveals that aggregate particles have the kind of organization of the hydrophobic and hydrophilic domains as they are present in HSA protein monomer molecules and aggregation of protein molecules causes the loss in the total solvent accessible surface area (SAS) is about 67% and the mean solvent content for these aggregates vary in the range of 0.37–0.55 volume fraction depending on the conformation of the monomer protein [175]. Therefore, at higher concentrations of protein, volume fraction of hydration water decreases due to formation of aggregates. In addition, proteins are THz transparent and as we increase the protein concentration, protein aggregates replace the water molecules and leads to lowering of total THz absorbance of the solution.

A method of analysis was adopted to analytically fit the data in the regime of higher concentrations of the protein to predict the relative concentrations of the monomer and aggregated particles. In this analysis, the value of  $\alpha_{hl}$ , which was estimated from the linear regime of the plot of  $\left(\frac{\alpha_{sol}}{\alpha_{bw}}\right)$  vs. [HSA] was used. Assuming that the THz absorption coefficient of the water molecules residing inside the aggregate as well as that constituting the hydration layer around the surface of the aggregate are similar to that constituting the hydration layer around the monomer protein molecule, Eq. (9) was revised to write Eq. (11), which provided a quantitative estimate of the relative numbers of the HSA molecules in the monomeric and aggregated forms in solution.

$$\left(\frac{\alpha_{sol}}{\alpha_{bw}}\right) = \left(\frac{\alpha_{hl}}{\alpha_{bw}}\right) (V_{hl}^{ag} + v_{hl}x + (1 - 0.08 V_{hl}^{ag} - Vv_{hl}x)) \quad (26)$$

Here,  $x$  is the concentration of monomer in the unit of  $1 \times 10^{-3} \text{ mol dm}^{-3}$  and  $V_{hl}^{ag}$  is the volume fraction of hydration water associated with the aggregates, both in the interstitial places as well as outside the aggregate constituting the hydration layer,  $v_{hl}$ , is the volume of hydration layer associated with one protein molecule.

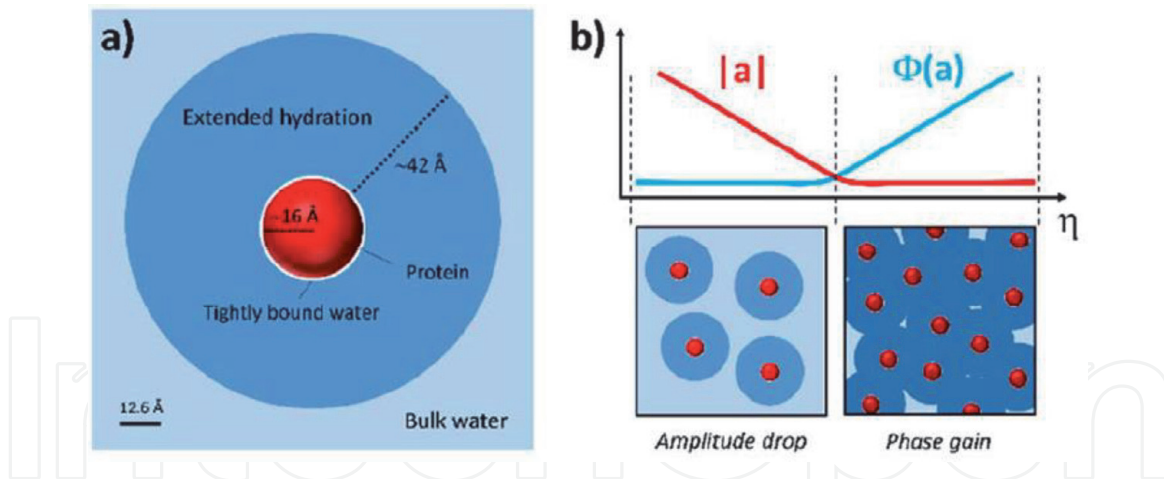


**Figure 7.**

(a) Cartoon of a human lysozyme protein (red sphere) in water. Water molecules tightly-bound to the protein surface (white), extended hydration layers (blue) and unperturbed bulk water (light blue). (b) Sketch of the evolution of the modulus and the phase of the induced dipole in a unit volume of solution versus protein concentration. The effect of phase gain at larger concentrations is represented by darker colors on the bottom right panel (adopted with permission from Ref. [170], Copyright (2017) American Chemical Society).

Manna et al. estimated the percentage of the number of HSA molecules, which exist as monomer (or dimer or trimer) in solution without being associated with aggregate formation, for each of the HSA concentrations used for THz absorption measurements [59]. We find that for the protein solution with its concentration of  $8 \times 10^{-4} \text{ mol dm}^{-3}$ , about 40% of the protein molecules exists as monomer (or dimer or trimer) in solution and 60% protein molecules are part of aggregates. The monomer (or dimer or trimer) concentration becomes  $<1\%$  at the protein concentration of  $2.6 \times 10^{-3} \text{ mol dm}^{-3}$ , i.e. nearly all the protein molecules are associated with aggregate formation. These calculations suggest that formation of aggregates at higher concentrations of protein may be the responsible factor for the turnover of the THz absorbance of the protein solution at  $\sim 6 \times 10^{-4} \text{ mol dm}^{-3}$  concentration.

The absorption coefficient of a complex system is the weighted sum of the absorption of its components. However, determination of the complex dielectric function of proteins in solution using THz-TDS spectroscopy allowed detailed analysis beyond what was possible from simple absorption measurements. Following this approach, Novelli et al. determined both the phase and amplitude of the induced dipole in the volume containing the protein and hydration water [170]. This result revealed that not only the amplitude of the induced dipole varied with the concentration of protein, but also its phase changed above a concentration threshold (**Figure 7**). They proposed a phenomenological model, which explained that the phase of the induced dipole in the protein-solvent interaction region began to vary when there was significant overlap between hydration layers of the neighboring protein. This result suggested that indirect electromagnetic protein-protein interactions could take place if mediated by the extended hydration layers surrounding each protein.

## 6. Conclusions and challenges ahead

THz spectroscopy, from its very inception, has mostly been used by scientists studying cosmology, condensed matter physics and materials. The huge absorption of water in this frequency range used to be treated as a drawback of this technique; however, for chemists and biologists this point serves as an advantage since all the biological function is somehow or other related to water dynamics. Due to its

inherent sensitivity to water hydrogen bonding dynamics, THz spectroscopy has become an indispensable tool for direct observation of fast and coupled biomolecule-water network. The initial studies by the groups of E. W. Heilweil, P.U. Jepsen, A. Marklez, C. Schmuttenmaer and M. Havenith in the late 1990s and early 2000s have established THz spectroscopy at a concrete platform to be recognized as a potential tool to label free detection of water dynamics in the vicinity of biomolecules, the effect being extended to several layers and remains practically undetected using conventional spectroscopic methods. The last decade has witnessed a huge leap towards exploiting this frequency window in biophysical studies, a few of such results have been depicted in this article. Now that the phenomenon has been established beyond any doubt, new sort of experimental studies, where the role of hydration in ultrafast processes (like electron transfer or proton transfer) could explicitly be determined, is the new challenge to the researchers.

### Author details

Rajib Kumar Mitra<sup>1\*</sup> and Dipak Kumar Palit<sup>2\*</sup>

1 Department of Chemical, Biological and Macromolecular Sciences, S.N. Bose National Centre for Basic Sciences, Kolkata, India

2 School of Chemical Sciences, UM-DAE Centre for Excellence in Basic Sciences, University of Mumbai, Mumbai, India

\*Address all correspondence to: [rajib@bose.res.in](mailto:rajib@bose.res.in) and [dkpalit@cbs.ac.in](mailto:dkpalit@cbs.ac.in)

### IntechOpen

© 2021 The Author(s). Licensee IntechOpen. This chapter is distributed under the terms of the Creative Commons Attribution License (<http://creativecommons.org/licenses/by/3.0>), which permits unrestricted use, distribution, and reproduction in any medium, provided the original work is properly cited. 

## References

- [1] Pal SK, Peon J, Bagchi B, Zewail AH. Biological water: Femtosecond dynamics of macromolecular hydration. *J. Phys. Chem. B* 2002;**106**:12376–12395
- [2] Nandi N, Bhattacharyya K, Bagchi B. Dielectric relaxation and solvation dynamics of water in complex chemical and biological systems. *Chem. Rev.* 2000;**100**:2013–2045
- [3] Ball P. Water as an Active Constituent in Cell Biology. *Chem. Rev.* 2008;**108**:74–108
- [4] Wolynes PG. Recent successes of the energy landscape theory of protein folding and function. *Quarterly Rev. Biophys.* 2005;**38**:405–410
- [5] Lynden-Bell R, Moris SC, Barrow JD, Finney JL, Harper JCL. *Water and Life: The Unique Properties of H<sub>2</sub>O* 2010. pp. Boca Raton: CRC Press
- [6] Bagchi B. *Water in Biological and Chemical Processes: From Structure and Dynamics to Function* 2013. pp. Cambridge: Cambridge University Press:
- [7] Hummer G, Tokmakoff A. Preface: Special Topic on Biological Water. *J. Chem. Phys.* 2014;**141**:22D101
- [8] Goodsell DS. *The Machinery of Life* 1993. pp. New York: Springer
- [9] Kunz Jr JD, Kauzmann W. Hydration of Proteins and Polypeptides. *Adv. Protein Chem.* 1974;**28**:239–345
- [10] Ball P. Water is an active matrix of life for cell and molecular biology. *Proc. Natl. Acad. Sci. U.S.A.* 2017;**114**:13327–13335
- [11] Levy Y, Onuchic JN. Water Mediation in Protein Folding and Molecular Recognition. *Ann. Rev. Biophys. Biomol. Struct.* 2006;**35**:389–415
- [12] Chaplin M. Do we underestimate the importance of water in cell biology? *Nat. Rev. Mol. Cell Biol.* 2006;**7**:861–866
- [13] Levitt M, Sharon R. Accurate simulation of protein dynamics in solution. *Proc. Natl. Acad. Sci. USA* 1988;**85**:7557–7561
- [14] Svergun D, Richard S, Koch MH, Sayers Z, Kuprin S, Zaccai G. Protein hydration in solution: Experimental observation by x-ray and neutron scattering. *Proc. Natl. Acad. Sci. USA* 1998; **95**:2267–2272
- [15] Smith JC, Merzel F, Verma CS, Fischer S. Protein Hydration Water: Structure and Thermodynamics. *J. Mol. Liq.* 2002;**101**:27–33
- [16] Uda Y, Zepeda S, Kaneko F, Matsuura Y, Furukawa Y. Adsorption-Induced Conformational Changes of Antifreeze Glycoproteins at the Ice/Water Interface. *J. Phys Chem. B* 2007; **111**:14355–14361
- [17] Yeh Y, Feeney RE. Antifreeze Proteins: Structures and Mechanisms of Function. *Chem. Rev.* 1996;**96**:601–618
- [18] Skalicky JJ, Sukumaran DK, Mills JL, Szyperski T. Toward Structural Biology in Supercooled Water. *J. Am. Chem. Soc.* 2000;**122**:3230–3231
- [19] Rick SW, Stuart SJ, Berne BJ. Dynamical fluctuating Charge Force Fields: Application to Liquid Water. *J. Chem. Phys.* 1994;**101**:6141
- [20] Persson E, Halle B. Cell Water Dynamics on Multiple Time Scales. *Proc. Natl. Acad. Sci. USA* 2008;**105**:6266–6271
- [21] Ojha L, Wilhelm MB, Murchie SL, McEwen AS, Wray JJ, et al. Spectral evidence for hydrated salts in recurring

- slope lineae on Mars. *Nature Geoscience* 2015;**8**: 829–832
- [22] Zhong D, Pal SK, Zewail AH. Biological water: A critique. *Chem. Phys. Lett.* 2011;**503**:1–11
- [23] Stillinger FH. Water Revisited. *Science* 1980;**209**:451–457
- [24] Chong SH, Ham S. Dynamics of Hydration Water Plays a Key Role in Determining the Binding Thermodynamics of Protein Complexes. *Sci. Rep.* 2017;**7**:8744
- [25] Gavrilov Y, Leuchter JD, Levy Y. On the coupling between the dynamics of protein and water. *Physical Chemistry Chemical Physics* 2017;**19**:8243–8257
- [26] Fogarty AC, Laage D. Water dynamics in protein hydration shells: The molecular origins of the dynamical perturbation. *J. Phys. Chem. B* 2014;**118**:7715–7729
- [27] Wang Z, Bertrand CE, Chiang WS, Fratini E, Baglioni P, et al. Inelastic X-ray scattering studies of the short-time collective vibrational motions in hydrated lysozyme powders and their possible relation to enzymatic function. *J. Phys. Chem. B* 2013;**117**:1186–1195
- [28] Frauenfelder H, Chen G, Berendzen J, Fenimore PW, Jansson H, et al. A unified model of protein dynamics. *Proc. Nat. Acad. Sci. USA* 2009;**106**:5129–5134
- [29] Tarek M, Tobias DJ. The dynamics of protein hydration water: A quantitative comparison of molecular dynamics simulations and neutron-scattering experiments. *Biophys. J.* 2000;**79**:3244–3257
- [30] Wood K, Plazanet M, Gabel F, Kessler B, Oesterhelt D, et al. Dynamics of hydration water in deuterated purple membranes explored by neutron scattering. *Eur. Biophys. J.* 2008;**37**: 619–626
- [31] Otting G, Liepinsh E. Protein Hydration Viewed by High-Resolution NMR Spectroscopy: Implications for Magnetic Resonance Image Contrast. *Acc. Chem. Res.* 1995;**28**:171–177
- [32] Jorge C, Marques BS, Valentine KG, Wand AJ. Characterizing Protein Hydration Dynamics Using Solution NMR Spectroscopy. *Methods Enzymol.* 2019;**615**:77–101
- [33] Camilloni C, Bonetti D, Morrone A, Giri R, Dobson CM, et al. Towards a Structural Biology of the Hydrophobic Effect in Protein Folding. *Sci. Rep.* 2016;**6**:28285
- [34] Moree B, Connell K, Mortensen RB, Liu CT, Benkovic SJ, Salafsky J. Protein Conformational Changes Are Detected and Resolved Site Specifically by Second-Harmonic Generation. *Biophys. J.* 2015;**109**:806–815
- [35] Vanzi F, Sacconi L, Cicchi R, Pavone FS. Protein conformation and molecular order probed by second-harmonic-generation microscopy. *J. Biomed. Opt.* 2012;**17**:060901
- [36] King JT, Kubarych KJ. Site-Specific Coupling of Hydration Water and Protein Flexibility Studied in Solution with Ultrafast 2D-IR Spectroscopy. *J. Am. Chem. Soc.* 2012;**134**:18705–18712
- [37] Ramos S, Horness RE, Collins JA, Haak D, Thielges MC. Site-specific 2D IR spectroscopy: a general approach for the characterization of protein dynamics with high spatial and temporal resolution. *Physical Chemistry Chemical Physics* 2019;**21**:780–788
- [38] Steinbach PJ, Brooks BR. Protein hydration elucidated by molecular dynamics simulation. *Proc. Natl. Acad. Sci. USA* 1993;**90**:9135–9139
- [39] Lagge D, Elsaesser T, Hynes JT. Perspective: Structure and ultrafast

- dynamics of biomolecular hydration shells. *Struct. Dyn.* 2017;**4**:044018
- [40] Titantah JT, Karttunen M. Long-time correlations and hydrophobe-modified hydrogen-bonding dynamics in hydrophobic hydration. *J. Am. Chem. Soc.* 2012;**134**:9362–9368
- [41] Mondal S, Mukherjee S, Bagchi B. Dynamical coupling between protein conformational fluctuation and hydration water: Heterogeneous dynamics of biological water. *Chem. Phys. Lett.* 2017;**683**:29–37
- [42] Nibali VC, Havenith M. New Insights into the Role of Water in Biological Function: Studying Solvated Biomolecules Using Terahertz Absorption Spectroscopy in Conjunction with Molecular Dynamics Simulations. *J. Am. Chem. Soc.* 2014;**136**:12800–12807
- [43] Xu Y, Havenith M. Perspective: Watching low-frequency vibrations of water in biomolecular recognition by THz spectroscopy. *J. Chem. Phys.* 2015; **143**:170901
- [44] Haller EE, E. B. 2000. *USA*
- [45] Keilmann F, Shastin VN, Till R. Pulse build-up of the germanium far-infrared laser. *App. Phys. Lett.* 1991;**58**:2205–2207
- [46] Shastin VN. Hot hole inter-sub-band transition p-Ge FIR laser. *Opt. Quantum Electronics* 1991;**23**:S111–S131
- [47] Bründermann E, Chamberlin DR, Haller EE. Thermal effects in widely tunable germanium terahertz lasers. *Appl. Phys. Lett.* 1998;**73**:2757
- [48] Pelka JB, Tyborb KR, Nietubyc R, Wrochna G. Applications of Free Electron Lasers in Biology and Medicine. *Acta Physica Polonica A.* 2010;**117**:427–432
- [49] Novelli F, Pestana LR, Bennett KC, Sebastiani F, Adams EM, et al. Strong anisotropy in liquid water upon librational excitation using terahertz laser fields. *J. Phys. Chem. B* 2020;**124**:4989–5001
- [50] Bye JW, Meliga S, Ferachou D, Cinque G, Zeitler JA, Falconer RJ. Analysis of the Hydration Water around Bovine Serum Albumin Using Terahertz Coherent Synchrotron Radiation. *J. Phys. Chem. A* 2014;**118**:83–88
- [51] Bergner A, Heugen U, Bründermann E, Schwaab G, Havenith M, et al. New p-Ge THz laser spectrometer for the study of solutions: THz absorption spectroscopy of water. *Rev. Sci. Instruments* 2005;**76**:063110
- [52] Ginsburg V, Frank I. Radiation of uniformly moving electron due to its transition from one medium into another. *J. Phys.* 1945; **9**:353
- [53] Naumenko GA, Aleinik AN, Aryshev AS, Kalinin BN, Potylitsyn AP, et al. Coherent transition and diffraction radiation from a bunched 6.1MeV electron beam. *Nuclear Instruments Methods Phys. Res. B* 2005;**227**:70–77
- [54] Kuroda R, Sei N, Yasumoto M, Toyokawa H, Ogawa H, et al. Generation of 0.1 THz coherent synchrotron radiation with compact S-band linac at AIST. *Infrared Phys. Technol.* 2008;**51**
- [55] Saisut J, Chaisueb N, Thongbai C, Rimjaem S. Coherent transition radiation from femtosecond electron bunches at the accelerator-based THz light source in Thailand. *Infrared Physics & Technology.* 2018; **92**, 387–391
- [56] Ter-Mikaelian ML. *High energy electromagnetic process in condensed media.* 1972. pp. New York: Wiley-Intersciencer
- [57] Ginzburg VL, Tsytovich VN, eds. 1990. *Transition radiation and transition scattering.* Bristol: Adam Hilger

- [58] Kuroda R, Toyokawa H, Sei N, Yasumoto M, Ogawa H, et al. Injector study for compact hard X-Ray source via laser Compton scattering. *Int. J. Mod. Phys.* 2007;**21**:488
- [59] Manna B, Nandi A, Tanaka M, Toyokawa H, Kuroda R, Palit DK. Effect of aggregation on hydration of HSA protein: Steady-state terahertz absorption spectroscopic study. *J. Chem. Sci.* 2020;**132**:8
- [60] Neu J, Schmittenmaer CA. Tutorial: An introduction to terahertz time domain spectroscopy (THz-TDS). *J. App. Phys.* 2018;**124**:231101
- [61] Roux J-F, Garet F, Coutaz J-L. 2014. Principles and applications of THz time domain spectroscopy. In *Physics and Applications of Terahertz Radiation*, ed. M Perenzoni, DJ Paul. Dordrecht: Springer. Number of
- [62] Wang C, Gong J, Xing O, Li Y, Liu F, et al. Application of terahertz time-domain spectroscopy in intracellular metabolite detection. *J. Biophotonics* 2010;**3**:641–645
- [63] Zeitler AJ, Philip TF, David AN, Pepper M, Keith GC, Rades T. Terahertz pulsed spectroscopy and imaging in the pharmaceutical setting—a review. *J. Pharm. Pharmacol.* 2007;**59**:209–223
- [64] Mittleman DM, Jakobsen RH, Neelamani R, Baraniuk RG, Nuss MC. Gas sensing using terahertz time-domain spectroscopy. *App. Phys. B* 1998;**67**:379
- [65] Cheville RA, Grischkowsky D. Far-infrared foreign and self-broadened rotational linewidths of high-temperature water vapor. *J. Op. Soc. Am. B* 1999;**16**:317
- [66] Kužel P, Petzelt J. Time-resolved terahertz transmission spectroscopy of dielectrics. *Ferroelectrics* 2000;**239**: 949
- [67] Jeon T-I, Grischkowsky D. Characterization of optically dense, doped semiconductors by reflection THz time domain spectroscopy. *App. Phys. Lett.* 1998;**72**:3032
- [68] Wilke I, Khazan M, Rieck CT, Kužel P, Kaiser T, et al. Terahertz surface resistance of high temperature superconducting thin films. *J. App. Phys.* 2000;**87**:2984
- [69] Plusquellic DF, Siegrist K, Heilweil EJ, Esenturk O. Applications of Terahertz Spectroscopy in Biosystems. *ChemPhysChem* 2007;**8**:2412–2431
- [70] Schmittenmaer CA. Exploring Dynamics in the Far-Infrared with Terahertz Spectroscopy. *Chem. Rev.* 2004;**104**:1759–1780
- [71] Beard MC, Turner GM, Schmittenmaer CA. Terahertz Spectroscopy. *J. Phys. Chem. B* 2002; **106**:7146–7159
- [72] Baxter JB, Guglietta GW. Terahertz Spectroscopy. *Anal. Chem.* 2011;**83**: 4342–4368
- [73] Yu L, Hao L, Meiqiong T, Jiaoqi H, Wei L, et al. The medical application of terahertz technology in non-invasive detection of cells and tissues: opportunities and challenges. *RSC Adv.* 2019 **9**:9354–9363
- [74] Yoon SA, Cha SH, Jun SW, Park SJ, Park J-Y, et al. Identifying different types of microorganisms with terahertz spectroscopy. *Biomed Opt Express.* 2020;**11**:406–416
- [75] Yomogida Y, Sato Y, Nozaki R, Mishina T, Nakahara J. Dielectric study of normal alcohols with THz time-domain spectroscopy. *J. Mol. Liq.* 2010; **154**:31–35
- [76] Sarkar S, Saha D, Banerjee S, Mukherjee A, Mandal P. Broadband terahertz dielectric spectroscopy of

- alcohols. Chem. Phys. Lett. 2017;**678**: 65–71
- [77] Kindt JT, Schmuttenmaer CA. Far-Infrared Dielectric Properties of Polar Liquids Probed by Femtosecond Terahertz Pulse Spectroscopy. J. Phys. Chem. 1996;**100**:10373–10379
- [78] Nee TW, Zwanzig R. Theory of dielectric relaxation in polar liquids. The Journal of Chemical Physics 1970;**52**: 6353–6363
- [79] Nandi N, Bhattacharyya K, Bagchi B. Dielectric relaxation and solvation dynamics of water in complex chemical and biological systems. Chemical Reviews 2000;**100**:2013–2046
- [80] Agieienko V, Horinek D, Buchner R. Hydration and self-aggregation of a neutral cosolute from dielectric relaxation spectroscopy and MD simulations: the case of 1, 3-dimethylurea. Physical Chemistry Chemical Physics 2017;**19**:219–230
- [81] Yuri Feldman PBI, Alexander Puzenko, Valerică Raicu. 2015. Elementary Theory of the Interaction of Electromagnetic Fields with Dielectric Materials. Oxford: Oxford University Press
- [82] Fröhlich H. *Theory of dielectrics: dielectric constant and dielectric loss* 1958. pp.: Clarendon Press
- [83] Bötcher C, Bordewijk P. 1978. Theory of Electric Polarization, vol. II, Dielectrics in Time-Dependent Fields. Elsevier Science
- [84] Feldman Y, Puzenko A, Ryabov Y. Dielectric Relaxation Phenomena in Complex Materials. Advances in chemical physics 2006;**133**:1
- [85] Schmidt DA, Birer Ö, Funkner S, Born B, Gnanasekaran R, et al. Rattling in the cage: ions as probes of sub-ps water network dynamics. J. Am. Chem. Soc. 2009;**131**:18512–18517
- [86] Funkner S, Niehues G, Schmidt DA, Heyden M, Schwaab G, et al. Watching the Low-Frequency Motions in Aqueous Salt Solutions: The Terahertz Vibrational Signatures of Hydrated Ions. J. Am. Chem. Soc. 2012;**134**:1030–1035
- [87] Smiechowski M, Sun J, Forbert H, Marx D. Solvation shell resolved THz spectra of simple aqua ions - distinct distance- and frequency-dependent contributions of solvation shells. Physical Chemistry Chemical Physics 2015;**17**:8323–8329
- [88] Sharma V, Boehm F, Seitz M, Schwaab G, Havenith M. From solvated ions to ion-pairing: a THz study of lanthanum(III) hydration. Physical Chemistry Chemical Physics 2013;**15**: 8383–8391
- [89] Sharma V, Boehm F, Schwaab G, Havenith M. The low frequency motions of solvated Mn(II) and Ni(II) ions and their halide complexes. Physical Chemistry Chemical Physics 2014;**16**: 25101–25110
- [90] Boehm F, Sharma V, Schwaab G, Havenith M. The low frequency modes of solvated ions and ion pairs in aqueous electrolyte solutions: iron(II) and iron(III) chloride. Physical Chemistry Chemical Physics 2015;**17**:19582–19591
- [91] Klinkhammer C, Boehm F, Sharma V, Schwaab G, Seitz M, Havenith M. Anion dependent ion pairing in concentrated ytterbium halide solutions. J. Chem. Phys. 2018; **148**:222802
- [92] Schwaab G, Sebastiani F, Havenith M. Ion Hydration and Ion Pairing as Probed by THz Spectroscopy. Angew. Chem. Int. Ed. 2019;**58**:3000–3013
- [93] Das Mahanta D, Samanta N, Mitra RK. The effect of monovalent cations on the collective dynamics of water and on a model protein. J. Mol. Liq. 2016;**215**:197–203

- [94] Schienbein P, Schwaab G, Forbert H, Havenith M, Marx D. Correlations in the Solute–Solvent Dynamics Reach Beyond the First Hydration Shell of Ions *J. Phys. Chem. Lett.* 2017;**8**:2373–2380
- [95] Walther M, Fischer BM, Jepsen PU. Noncovalent intermolecular forces in polycrystalline and amorphous saccharides in the far infrared. *Chem. Phys.* 2003;**261–268**:261–268
- [96] Shiraga K, Adachi A, Nakamura M, Tajima T, Ajito K, Ogawa Y. Characterization of the hydrogen-bond network of water around sucrose and trehalose: Microwave and terahertz spectroscopic study. *J. Chem. Phys.* 2017;**146**:105102
- [97] Heugen U, Schwaab G, Bründermann E, Heyden M, Yu X, et al. Solute-induced retardation of water dynamics probed directly by terahertz spectroscopy. *Proc. Natl. Acad. Sci. USA* 2006;**103**:12301–12306
- [98] Lee D-K, Kang J-H, Lee J-S, Kim H-S, Kim C, et al. Highly sensitive and selective sugar detection by terahertz nano-antennas. *Sci. Rep.* 2015; **5**:15459
- [99] Sajadi M, Berndt F, Richter C, Gerecke M, Mahrwald R, Ernsting NP. Observing the Hydration Layer of Trehalose with a Linked Molecular Terahertz Probe. *J. Phys. Chem. Lett.* 2014;**5**:1845–1849
- [100] Heyden M, Bründermann E, Heugen U, Niehues G, Leitner DM, Havenith M. Long range influence of carbohydrates on the solvation dynamics of water - Answers from THz absorption measurements and molecular modeling simulations. *J. Am. Chem. Soc.* 2008;**130**:5773–5779
- [101] Samanta N, Das Mahanta D, Mitra RK. Does Urea Alter the Collective Water Structure: A Dielectric Relaxation Study in THz Region. *Chem. Asian J.* 2014;**9**:3457–3463
- [102] England JL, Haran G. Role of solvation effects in protein denaturation: From thermodynamics to single molecules and back. *Ann. Rev. Phys. Chem.* 2011;**62**:257–277
- [103] Jui-Yoa Chang J-Y. Structural Heterogeneity of 6 M GdmCl-Denatured Proteins: Implications for the Mechanism of Protein Folding. *Biochemistry* 2009;**48**:9340–9346
- [104] Das Mahanta D, Samanta N, Mitra RK. The Decisive Role of Hydrophobicity on the Effect of Alkylammonium Chlorides on Protein Stability: A Terahertz Spectroscopic Finding. *J. Phys Chem. B* 2017;**121**:7777–7785
- [105] Niehues G, Heyden M, Schmidt DA, Havenith M. Exploring hydrophobicity by THz absorption spectroscopy of solvated amino acids. *Faraday Discussions* 2011;**150**:193–207
- [106] Sun J, Niehues G, Forbert H, Decka D, Schwaab G, et al. Understanding THz Spectra of Aqueous Solutions: Glycine in Light and Heavy Water. *J. Am. Chem. Soc.* 2014;**136**: 5031–5038
- [107] Esser A, Forbert H, Sebastiani F, Schwaab G, Havenith M, Marx D. Hydrophilic Solvation Dominates the Terahertz Fingerprint of Amino Acids in Water. *J. Phys. Chem. B* 2018;**122**:1453–1459
- [108] Shiraga K, Suzuki T, Kondo N, Ogawa Y. Hydration and hydrogen bond network of water around hydrophobic surface investigated by terahertz spectroscopy. *J. Chem. Phys.* 2014;**141**: 235103
- [109] Samanta N, Das Mahanta D, Choudhury S, Barman A, Mitra RK. Collective Hydration Dynamics in Some

- Amino Acid Solutions: A Combined GHz-THz Spectroscopic Study. *J. Chem. Phys.* 2017;**146**:125101
- [110] Born B, Weingartner H, Bruendermann E, Havenith M. Solvation dynamics of model peptides probed by terahertz spectroscopy. Observation of the onset of collective network motions. *J. Am. Chem. Soc.* 2009;**131**:3752–3755
- [111] Das Mahanta D, Islam SI, Choudhury S, Das DK, Mitra RK, Barman A. Contrasting hydration dynamics in DME and DMSO aqueous solutions: A combined optical pump-probe and GHz-THz dielectric relaxation investigation. *J. Mol. Liq.* 2019;**290**:111194
- [112] Luong TQ, Verma PK, Mitra RK, Havenith M. Onset of Hydrogen Bonded Collective Network of Water in 1,4-Dioxane. *J. Phys. Chem. A* 2011;**115**:14462–14469
- [113] Das Mahanta D, Patra A, Samanta N, Luong TQ, Mukherjee B, Mitra RK. Non-monotonic dynamics of water in its binary mixture with 1,2-dimethoxy ethane: A combined THz spectroscopic and MD simulation study. *J. Chem. Phys.* 2016;**145**:164501
- [114] Boehm F, Schwaab G, Havenith M. Mapping Hydration Water around Alcohol Chains by THz Calorimetry. *Angew. Chem. Int. Ed.* 2017;**56**:9981–9985
- [115] Born B, Kim SJ, Ebbinghaus S, Gruebele M, Havenith M. The terahertz dance of water with the proteins: the effect of protein flexibility on the dynamical hydration shell of ubiquitin. *Faraday Discussions* 2009;**141**:161–173
- [116] Heyden M, Havenith M. Combining THz spectroscopy and MD simulations to study protein-hydration coupling. *Methods* 2010;**52**:74–83
- [117] Ebbinghaus S, Kim SJ, Heyden M, Yu X, Gruebele M, et al. Protein Sequence- and pH-Dependent Hydration Probed by Terahertz Spectroscopy. *J. Am. Chem. Soc.* 2008;**130**:2374–2375
- [118] Vondracek H, Dielmann-Gessner J, Lubitz W, Knipp M, Havenith M. THz absorption spectroscopy of solvated  $\beta$ -lactoglobulin. *J. Chem. Phys.* 2014;**141**:22D534
- [119] Heyden M, Sun J, Funkner S, Mathias G, Forbert H, et al. Dissecting the THz spectrum of liquid water from first principles via correlations in time and space. *Proc. Natl. Acad. Sci. USA* 2010;**107**:12068–12073
- [120] Grossman M, Born B, Heyden M, Tworowski D, Fields GB, et al. Correlated structural kinetics and retarded solvent dynamics at the metalloprotease active site. *Nat. Struct. Mol. Biol.* 2011;**18**:1102–1108
- [121] Adams EM, Lampret O, Koenig B, Happe T, Havenith M. Solvent dynamics play a decisive role in the complex formation of biologically relevant redox proteins. *Physical Chemistry Chemical Physics* 2020;**22**:7451–7459
- [122] He Y, Ku PI, Knab JR, Chen JY, Markelz AG. Protein Dynamical Transition Does Not Require Protein Structure. *Phys. Rev. Lett.* 2008;**101**:178103
- [123] He Y, Chen J-Y, Knab JR, Zheng W, Markelz AG. Evidence of Protein Collective Motions on the Picosecond Timescale. *Biophys. J.* 2011;**100**:1058–1065
- [124] Acbas G, Niessen KA, Snell EH, Markelz AG. Optical measurements of long-range protein vibrations. *Nat. Commun.* 2014;**5**:4076
- [125] Turton DA, Senn HM, Harwood T, Laphorn AJ, Ellis EM, Wynne K.

Terahertz underdamped vibrational motion governs protein-ligand binding in solution. *Nat. Commun.* 2014;**5**:3999

[126] Niessen KA, Xu M, George DK, Chen MC, Ferré-D'Amaré AR, et al. Protein and RNA dynamical fingerprinting. *Nat. Commun.* 2019;**10**:1026

[127] Sun Y, Du P, Lu X, Xie P, Qian Z, et al. Quantitative characterization of bovine serum albumin thin-films using terahertz spectroscopy and machine learning methods. *Biomed. Opt. Express* 2018;**9**:2917–2929

[128] Sun Y, Junlan Zhong J, Zhang C, Zuo J, Pickwell-MacPherson E. Label-free detection and characterization of the binding of hemagglutinin protein and broadly neutralizing monoclonal antibodies using terahertz spectroscopy. *J. Biomed. Optic* 2015;**20**:037006

[129] Sun Y, Zhang Y, Pickwell-MacPherson E. Investigating Antibody Interactions with a Polar Liquid Using Terahertz Pulsed Spectroscopy. *Biophys. J.* 2011;**100**:225–231

[130] Sun Y, Zhu Z, Chen S, Balakrishnan J, Abbott D, et al. Observing the Temperature Dependent Transition of the GP2 Peptide Using Terahertz Spectroscopy. *PloS one* 2012;**7**: e50306

[131] Markelz AG, Roitberg A, Heilweil EJ. Pulsed terahertz spectroscopy of DNA, bovine serum albumin and collagen between 0.1 and 2.0 THz. *Chem. Phys. Lett.* 2000;**320**: 42–48

[132] Fischer BM, Walther M, Jepsen PU. Far-infrared vibrational modes of DNA components studied by terahertz time-domain spectroscopy. *Phys. Med. Biol.* 2002;**47**:3807–3814

[133] Brucherseifer M, Nagel M, Bolivar PH, Kurz H. Label-free probing of the binding state of DNA by time-

domain terahertz sensing. *Appl. Phys. Lett.* 2000;**77**:4049–4051

[134] Arora A, Luong TQ, Kruger M, Kim YJ, Nam C-H, et al. Terahertz-time domain spectroscopy for the detection of PCR amplified DNA in aqueous solution. *Analyst* 2012;**137**:575

[135] Tang M, Zhang M, Yan S, Xia L, Yang Z, et al. Detection of DNA oligonucleotides with base mutations by terahertz spectroscopy and microstructures. *PLoS One* 2018;**13**: e0191515

[136] Polley D, Patra A, Mitra RK. Dielectric relaxation of the extended hydration sheathe of DNA in the THz frequency region. *Chem. Phys. Lett.* 2013 **586**:143–147

[137] Tielrooij KJ, Paparo D, Piatkowski L, Bakker HJ, Bonn M. Dielectric Relaxation Dynamics of Water in Model Membranes Probed by Terahertz Spectroscopy. *Biophys. J.* 2009;**97**:2484–2492

[138] Yamamoto N, Andachi T, Tamura A, Tominaga K. Temperature and Hydration Dependence of Low-Frequency Spectra of Lipid Bilayers Studied by Terahertz Time-Domain Spectroscopy. *J. Phys. Chem. B* 2015; **119**:9359–9368

[139] Yamamoto N, Ito S, Nakanishi M, Chatani E, Inoue K, et al. Effect of Temperature and Hydration Level on Purple Membrane Dynamics Studied Using Broadband Dielectric Spectroscopy from Sub-GHz to THz Regions. *J. Phys. Chem. B* 2018;**122**:1367–1377

[140] Kadomura Y, Yamamoto N, Tominaga K. Broadband dielectric spectroscopy from sub GHz to THz of hydrated lipid bilayer of DMPC. *Eur. Phys. J. E* 2019 **42**:139

[141] Pal S, Samanta N, Das Mahanta D, Mitra RK, Chattopadhyay A. Effect of

- Phospholipid Headgroup Charge on the Structure and Dynamics of Water at the Membrane Interface: A Terahertz Spectroscopic Study. *J. Phys. Chem. B* 2018;**122**:5066–5074
- [142] Kim SJ, Born B, Havenith M, Gruebele M. Real-time detection of protein-water dynamics upon protein folding by terahertz absorption spectroscopy. *Angew. Chem. Int. Ed.* 2008;**47**:6486–6489
- [143] Luong TQ, Verma PK, Mitra RK, Havenith M. Do Hydration Dynamics Follow the Structural Perturbation during Thermal Denaturation of a Protein: A Terahertz Absorption Study *Biophys. J.* 2011;**101**:925–933
- [144] Luong TQ, Xu Y, Bründermann E, Leitner DM, Havenith M. Hydrophobic collapse induces changes in the collective protein and hydration low frequency modes. *Chem. Phys. Lett.* 2016;**651**:1–7
- [145] Wirtz H, Schäfer S, Hoberg C, Reid KM, Leitner DM, Havenith M. Hydrophobic Collapse of Ubiquitin Generates Rapid Protein–Water Motions. *Biochemistry* 2018;**57**:3650–3657
- [146] Li X, Fu X, Liu J, Du Y, Hong Z. Investigation of thermal denaturation of solid bovine serum albumin by terahertz dielectric spectroscopy. *J. Mol. Struct.* 2013;**1049**:441–445
- [147] Zang Z, Yan S, Han X, Wei D, Cui H-L, Du C. Temperature- and pH-dependent protein conformational changes investigated by terahertz dielectric spectroscopy. *Infrared Phys. Technol.* 2019;**98**:260–265
- [148] Cao C, Serita K, Kitagishi K, Murakami H, Zhang Z-H, Tonouchi M. Terahertz Spectroscopy Tracks Proteolysis by a Joint Analysis of Absorbance and Debye Model. *Biophys. J.* (DOI: 10.1016/j.bpj.2020.11.003) 2020
- [149] Samanta N, Luong TQ, Das Mahanta D, Mitra RK, Havenith M. Effect of Short Chain Poly(ethylene glycol)s on the Hydration Structure and Dynamics around Human Serum Albumin. *Langmuir* 2016;**32**:831–837
- [150] Das DK, Patra A, Mitra RK. Preferential solvation of lysozyme in dimethyl sulfoxide/water binary mixture probed by terahertz spectroscopy. *Biophys. Chem.* 2016;**216**:31–36
- [151] Das DK, Das Mahanta D, Mitra RK. Non-monotonous Hydration Behaviour of Bovine Serum Albumin in Alcohol-Water Binary Mixtures: A THz Spectroscopic Investigation. *ChemPhysChem* 2017;**18**:749–754
- [152] Stefani M, Dobson CM. Protein aggregation and aggregate toxicity: new insights into protein folding, misfolding diseases and biological evolution. *J. Mol. Med.* 2003;**81**:678–699
- [153] Ross CA, Poirier MA. Protein aggregation and neurodegenerative disease. *Nat. Med.* 2004;**10**:S10-S17
- [154] Zhang SG. Fabrication of Novel Biomaterials through Molecular Self-Assembly. *Nat. Biotechnol.* 2003;**21**:1171–1178
- [155] Gotz J, Ittner LM, Lim YA. Common features between diabetes mellitus and Alzheimer’s disease. *Cellular Mol. Lifesci.* 2009;**66**:1321–1325
- [156] J.C. R, Outeiro TF, Conway KA, Ding TT, Volles MJ, et al. Interactions among alpha-synuclein, dopamine, and biomembranes-some clues for understanding neurodegeneration in Parkinson’s disease. *J. Mol. Neurosci.* 2004;**23**:23–33
- [157] Sa’ a P, Harris DA, Cervenakova L. Mechanisms of prion-induced neurodegeneration. *Expt. Rev. Mol. Med.* 2016;**18**:e5

- [158] Nayak A, Dutta AK, Belfort G. Surface-enhanced nucleation of insulin amyloid fibrillation. *Biochem. Biophysics Res. Comm.* 2008;**369**:303–307
- [159] Chiti F, Dobson CM. Protein misfolding, functional amyloid, and human disease. *Annu. Rev. Biochem.* 2006;**75**:333–366
- [160] Fink AL. Protein aggregation: folding aggregates, inclusion bodies and amyloid. *Folding & Design* 1998;**3**:R9-R23
- [161] Poulson BG, Szczepski K, Lachowicz JI, Jaremko L, Emwas AH, Jaremko M. Aggregation of biologically important peptides and proteins: inhibition or acceleration depending on protein and metal ion concentrations. *RSC Adv.* 2020;**10**:215–227
- [162] Chong S-H, Ham S. Interaction with the Surrounding Water Plays a Key Role in Determining the Aggregation Propensity of Proteins. *Angew. Chem. Int. Ed.* 2014;**53**:3961–3964
- [163] Chong SH, Ham S. Impact of chemical heterogeneity on protein self-assembly in water. *Proc. Natl. Acad. Sci. USA* 2012;**109**:7636–7641
- [164] Kodaka M. Interpretation of concentration-dependence in aggregation kinetics. *Biophys. Chem* 2004;**109**:325–332
- [165] Bhattacharya A, Prajapati R, Chatterjee S, Mukherjee TK. ConcentrationDependent Reversible Self-Oligomerization of Serum Albumins through Intermolecular  $\beta$ -Sheet Formation. *Langmuir* 2014;**30**: 14894–14904
- [166] Huang K, Kingsley CN, Sheil R, Cheng C, Bierma JB, et al. Stability of protein-specific hydration shell on crowding. *J. Am. Chem. Soc.* 2016;**138**: 5392–5402
- [167] Molodenskiy D, Shirshin E, Tikhonova T, Gruzinov A, Petersa G, Spinozzi F. Thermally induced conformational changes and protein-protein interactions of bovine serum albumin in aqueous solution under different pH and ionic strengths as revealed by SAXS measurements. *Physical Chemistry Chemical Physics* 2017;**19**:17143–17155
- [168] Baler K, Martin OA, Carignano MA, Ameer GA, Vila JA, Szleifer I. Electrostatic Unfolding and Interactions of Albumin Driven by pH Changes: A Molecular Dynamics Study. *J. Phys. Chem. B* 2014;**118**:921–930
- [169] Ebbinghaus S, Kim SJ, Heyden M, Yu X, Heugen U, et al. An extended dynamical hydration shell around proteins. *Proc. Natl. Acad. Sci. USA* 2007;**104**:20749–20752
- [170] Novelli F, Ostovar Pour SO, Tollerud J, Roozbeh A, Appadoo DRT, et al. Time-Domain THz Spectroscopy Reveals Coupled Protein–Hydration Dielectric Response in Solutions of Native and Fibrils of Human Lysozyme. *J. Phys. Chem. B* 2017;**121**:4810–4816
- [171] Chong S-H, Ham S. Distinct Role of Hydration Water in Protein Misfolding and Aggregation Revealed by Fluctuating Thermodynamics Analysis. *Acc. Chem. Res.* 2015, 4;**48**:956–965
- [172] Dorbez-Sridi R, Cortès R, Mayer E, Pin S. X-ray scattering study of the structure of water around myoglobin for several levels of hydration. *J. Chem. Phys.* 2002;**116**:7269
- [173] Sushko O, Dubrovka R, Donnana RS. Sub-terahertz spectroscopy reveals that proteins influence the properties of water at greater distances than previously detected. *J. Chem. Phys.* 2015;**142**:055101
- [174] Patro SY, Przybycien TM. Simulations of reversible protein aggregate and crystal structure. *Biophys. J.* 1996;**70**:2888–2902

[175] Jachimska B, Wasilewska M, Adamczyk Z. Characterization of Globular Protein Solutions by Dynamic Light Scattering, Electrophoretic Mobility, and Viscosity Measurements. *Langmuir* 2008;**24**:6866–6872

IntechOpen

IntechOpen